

ผลของความขึ้นสัมพัทธ์ต่อสมรรถนะของแพลทินัม/ซีโอไลต์-โคโตซานเมมเบรนในเซลล์เชื้อเพลิง
พีอีเอ็ม



นางสาวอัครินทร์ อังคตวีรัตน์

ศูนย์วิทยทรัพยากร

วิทยานิพนธ์นี้เป็นส่วนหนึ่งของการศึกษาตามหลักสูตรปริญญาวิทยาศาสตรมหาบัณฑิต

สาขาวิชาปิโตรเคมีและวิทยาศาสตร์พอลิเมอร์

คณะวิทยาศาสตร์ จุฬาลงกรณ์มหาวิทยาลัย

ปีการศึกษา 2552

ลิขสิทธิ์ของจุฬาลงกรณ์มหาวิทยาลัย

EFFECTS OF RELATIVE HUMIDITY ON PERFORMANCE OF Pt/ZEOLITE-CHITOSAN
MEMBRANE IN PEM FUEL CELL



Miss Agkarapin Angkatreerat

ศูนย์วิทยทรัพยากร

A Thesis Submitted in Partial Fulfillment of the Requirements

for the Degree of Master of Science Program in Petrochemistry and Polymer Science

Faculty of Science


Chulalongkorn University

Academic Year 2009

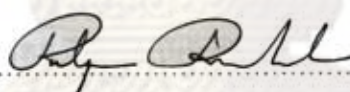
Copyright of Chulalongkorn University

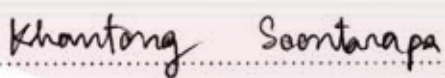
Thesis Title EFFECTS OF RELATIVE HUMIDITY ON PERFORMANCE OF
Pt/ZEOHITE-CHITOSAN MEMBRANE IN PEM FUEL CELL
By Miss Agkarapin Agkatreerat
Field of Study Petrochemistry and Polymer Science
Thesis Advisor Associate Professor Khantong Soontarapa, Ph.D.

Accepted by the Faculty of Science, Chulalongkorn University in Partial
Fulfillment of the Requirements for the Master's Degree

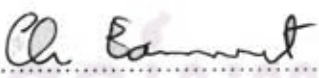

..... Dean of the Faculty of Science
(Professor Supot Hannongbua, Dr.rer. nat.)

THESIS COMMITTEE


..... Chairman
(Professor Pattarapan Prasassarakich, Ph.D.)


..... Thesis Advisor
(Associate Professor Khantong Soontarapa, Ph.D.)


..... Examiner
(Assistant Professor Vorawee Hoven, Ph.D.)


..... External Examiner
(Chutima Eamchotchawalit, Ph.D.)

อัครพันธ์ อัครวีรัตน์: ผลของความชื้นสัมพัทธ์ต่อสมรรถนะของแพลทินัม/ซีโอไลต์-ไคโตซานเมมเบรน ในเซลล์เชื้อเพลิงพีอีเอ็ม (EFFECTS OF RELATIVE HUMIDITY ON PERFORMANCE OF P/ZEOLITE-CHITOSAN MEMBRANE IN PEM FUEL CELL) อ. ที่ปรึกษาวิทยานิพนธ์หลัก: รองศาสตราจารย์ ดร. ชันทอง สุนทรภา, 97 หน้า.

งานวิจัยนี้ได้ศึกษาผลของความชื้นสัมพัทธ์ต่อสมรรถนะของแพลทินัม/ซีโอไลต์-ไคโตซานเมมเบรนในเซลล์เชื้อเพลิงพีอีเอ็ม ชนิดของเมมเบรนที่ศึกษาได้แก่ เมมเบรนไคโตซานไม่เชื่อมขวาง เมมเบรนไคโตซานเชื่อมขวาง และเมมเบรนเชื่อมขวางไคโตซานโดยปด้วยสารละลายกรดซัลฟิวริกเข้มข้นร้อยละ 2 โดยน้ำหนัก ปริมาณซีโอไลต์ชนิดเอที่ศึกษาตั้งแต่อัตราส่วนร้อยละ 0 ถึง 30 โดยน้ำหนักของไคโตซาน พบว่าเมื่อปริมาณซีโอไลต์เพิ่มขึ้นความสามารถในการแลกเปลี่ยนไอออนและค่าการนำโปรตอนมีค่าเพิ่มขึ้น แต่ค่าความสามารถในการทนต่อแรงดึงและค่าการซึมผ่านแก๊สไฮโดรเจนลดลง ค่าการนำโปรตอนของเมมเบรนเชื่อมขวางคอมโพสิตไคโตซาน-ซีโอไลต์ร้อยละ 30 ให้ค่าการนำโปรตอนในแนวระนาบ ณ อุณหภูมิ 60 องศาเซลเซียส เท่ากับ 0.043 ± 0.006 ซีเมนส์ต่อเซนติเมตร และเมื่อผ่านการโดยปด้วยสารละลายกรดซัลฟิวริกเข้มข้นร้อยละ 2 โดยน้ำหนัก มีค่าสูงขึ้นเป็น 0.123 ± 0.024 ซีเมนส์ต่อเซนติเมตร หลังการเคลือบตัวเร่งปฏิกิริยาแพลทินัมด้วยเทคนิคการเคลือบโดยไม่ใช้ไฟฟ้า ที่อุณหภูมิ 60 องศาเซลเซียส นาน 90 นาที เมมเบรนเชื่อมขวางคอมโพสิตไคโตซาน-ซีโอไลต์ร้อยละ 30 ที่ผ่านการโดยปให้ค่าการนำโปรตอนในแนวระนาบเท่ากับ 0.312 ± 0.008 ซีเมนส์ต่อเซนติเมตร ในการศึกษาสมรรถนะเซลล์เชื้อเพลิงเดี่ยวที่อุณหภูมิ 30 องศาเซลเซียส พบว่าเมมเบรนเชื่อมขวางคอมโพสิตไคโตซาน-ซีโอไลต์ร้อยละ 30 ให้ค่าความหนาแน่นกระแสไฟฟ้าที่ 0.5 โวลท์ เพิ่มขึ้นจาก 2.9 ± 0.1 มิลลิแอมแปร์ต่อตารางเซนติเมตรที่สภาวะทำให้แก๊สป้อนขึ้นจากภายนอกจนอิ่มตัวทั้งสองด้าน (ความชื้นสัมพัทธ์ที่ฝั่งแอโนด-แคโทดเป็น 100%-100%) เป็น 5.1 ± 0.1 มิลลิแอมแปร์ต่อตารางเซนติเมตร เมื่อไม่มีการทำให้แก๊สป้อนขึ้นจากภายนอกทั้งสองด้าน (ความชื้นสัมพัทธ์ที่ฝั่งแอโนด-แคโทดเป็น 0%-0%) ในบรรดาเมมเบรนฐานไคโตซานที่ศึกษาพบว่าหน่วยเมมเบรนอิเล็กโทรดซึ่งเตรียมจากเมมเบรนเชื่อมขวางคอมโพสิตไคโตซาน-ซีโอไลต์ร้อยละ 30 ที่ผ่านการโดยปให้สมรรถนะเซลล์เชื้อเพลิงดีที่สุด โดยให้ค่าความหนาแน่นกระแสไฟฟ้าที่ 0.5 โวลท์ และไม่มีการทำให้แก๊สป้อนขึ้นจากภายนอกทั้งสองทดสอบที่อุณหภูมิ 30, 60 และ 90 องศาเซลเซียส เท่ากับ 9.5 ± 0.01 , 9.8 ± 0.01 และ 10.1 ± 0.01 มิลลิแอมแปร์ต่อตารางเซนติเมตร ตามลำดับ

สาขาวิชา วิศวกรรมและวิทยาศาสตร์พอลิเมอร์ ลายมือชื่อนิสิต อัครพันธ์ อัครวีรัตน์

ปีการศึกษา 2552 ลายมือชื่อ อ. ที่ปรึกษาวิทยานิพนธ์หลัก ชันทอง สุนทรภา

5172549623: MAJOR PETROCHEMISTRY AND POLYMER SCIENCE

KEYWORDS : CHITOSAN MEMBRANE / PERFORMANCE / PEM FUEL CELL / HUMIDITY

AGKARAPIN ANGKATREERAT: EFFECTS OF RELATIVE HUMIDITY ON PERFORMANCE OF Pt/ZEOCLITE-CHITOSAN MEMBRANE IN PEM FUEL. THESIS
ADVISOR: ASSOC.PROF. KHANTONG SOONTARAPA, Ph.D., 97 pp.

This research studied the effects of relative humidity on performance of Pt/zeolite-chitosan membrane in PEM fuel cell. The studied membranes were uncrosslinked chitosan, crosslinked chitosan and doped crosslinked chitosan membranes. The doping solution was 2% by weight of sulfuric acid. Zeolite A was incorporated in the range of 0-30% by weight of chitosan. It was found that the ion exchange capacity and proton conductivity was increased with zeolite content however the tensile strength and gas permeability was decreased. The proton conductivity in planar view at 60°C of 30% crosslinked chitosan-zeolite membranes was 0.043±0.006 S/cm and increased to 0.123±0.024 S/cm in doped membranes. After Pt plating by electroless technique at 60°C for 90 min, the proton conductivity of 30% doped crosslinked chitosan-zeolite membrane was increased to 0.312±0.008 S/cm. In single cell testing at 30°C, the current density at 0.5 V of 30% crosslinked chitosan-zeolite membrane was increased from 2.9±0.1 mA/cm² at fully hydration (RH at anode-cathode sides are 100%-100%) to 5.1±0.1 mA/cm² for zero hydration (RH at anode-cathode sides are 0%-0%) at both sides. Amongst the studied chitosan based membranes, it was found that the 30% doped crosslinked chitosan-zeolite membrane provided the best performance. The current densities at 0.5 V without external humidifier at 30, 60 and 90°C were 9.5±0.01, 9.8±0.01, and 10.1±0.01 mA/cm², respectively.

Field of Study: Petrochemistry and Polymer Science Student's Signature อ.กษิณี อ.กษิณี

Academic Year: 2009 Advisor's Signature อ.กษิณี อ.กษิณี

ACKNOWLEDGEMENTS

This is a pleasure to thank many people who made this thesis possible. It is difficult to overstate her gratitude to her adviser, Associate Professor Dr. Khantong Soontarapa for her constructive advice, initial instigation, worthy comments, sound advice, good teaching, and lots of good ideas. The author would have been lost without her.

The author also would like to express her appreciation to Professor Dr. Pattarapan Prasassarakich, Assistant Professor Dr. Vorawee Hoven and Dr. Chutima Eamchotchawalit for serving as the chairman, examiner and external examiner, respectively, for their valuable comments and suggestions.

The greatest thanks are extended to the Graduate School, Chulalongkorn University and Petrochemistry and Polymer Science, Faculty of Science, Chulalongkorn University for their research grant. In addition, thanks are also extended to the Center for Petroleum, Petrochemicals, and Advanced Materials, the Thailand Research Fund and the 90th Anniversary of chulalongkorn university fund (Ratchadaphiseksomphot Endowment Fund) for the support of the research fund.

Special thanks to her friends for friendship and deserve special mentions.

The author wish to deep thanks her family for providing a loving environment for her.

Without them, the author dream would never have been able to achieve this goal.

ศูนย์วิจัยทรัพยากร
จุฬาลงกรณ์มหาวิทยาลัย

CONTENTS

	Page
ABSTRACT (Thai).....	iv
ABSTRACT (English).....	v
ACKNOWLEDGEMENTS.....	vi
CONTENTS.....	vii
LIST OF TABLES.....	x
LIST OF FIGURES.....	xi
CHAPTER I INTRODUCTION.....	1
1.1 Statement of Problem.....	1
1.2 Objective.....	1
1.3 Scope of investigation.....	2
CHAPTER II THEORY AND LITERATURE REVIEW.....	3
2.1 Fuel Cell Basics.....	3
2.1.1 Alkaline Fuel Cells (AFC).....	3
2.1.2 Molten Carbonate Fuel Cells (MCFC)	4
2.1.3 Solid Oxide Fuel Cells (SOFC).....	5
2.1.4 Phosphoric Acid Fuel Cells (PAFC).....	6
2.1.5 Direct Methanol Fuel Cells (DMFC).....	7
2.1.6 Proton exchange membrane fuel cell (PEMFC)	8
2.2 Principle of proton exchange membrane fuel cell (PEMFC).....	9
2.3 The composition of proton exchange membrane fuel cell.....	10
2.3.1 Current Collector Plate.....	10
2.3.2 Membrane Electrode Assembly (MEA).....	10
2.4 Chitin and Chitosan.....	14
2.5 Zeolite.....	15
2.6 Preparation of Membrane electrode assembly (MEA).....	17
2.6.1 Gas diffusion layer/Catalyst assembly.....	17

	Page
2.6.2 Membrane/Catalyst assembly.....	18
2.7 Electroless deposition.....	19
2.8 Effects of parameters on the performance of PEMFC.....	21
2.8.1 Effect of water on the performance of PEMFC.....	21
2.8.2 Effect of temperature on PEMFC performance.....	22
2.9 Polarization.....	23
2.9.1 Activation Polarization or Chemical Polarization.....	25
2.9.2 Resistance polarization.....	25
2.9.3 Concentration Polarization.....	26
2.10 Humidity.....	26
2.11 Related works.....	27
CHAPTER III EXPERIMENTAL.....	29
3.1 Chemicals and Materials.....	29
3.2 Instruments.....	29
3.3 Analytical Instruments.....	31
3.4 Methodology.....	31
3.4.1 Membrane Preparation.....	31
3.4.2 Tensile strength test.....	32
3.4.3 Ion exchange capacity test.....	33
3.4.4 Constant Pressure Gas Permeability Test.....	34
3.4.5 Membrane Proton Conductivity by Four Probe Method.....	35
3.4.6 Coating of Catalyst Layer on the Membrane by Electroless Plating Technique	36
3.4.7 Characterizations of Plated Membrane.....	37
3.4.8 Preparation of Membrane/Electrode Assembly (MEA).....	37
3.4.9 Proton Conductivity in a Single Cell.....	38
3.4.10 Performance Testing of a Single Fuel Cell.....	38
CHAPTER IV RESULTS AND DISCUSSION.....	40

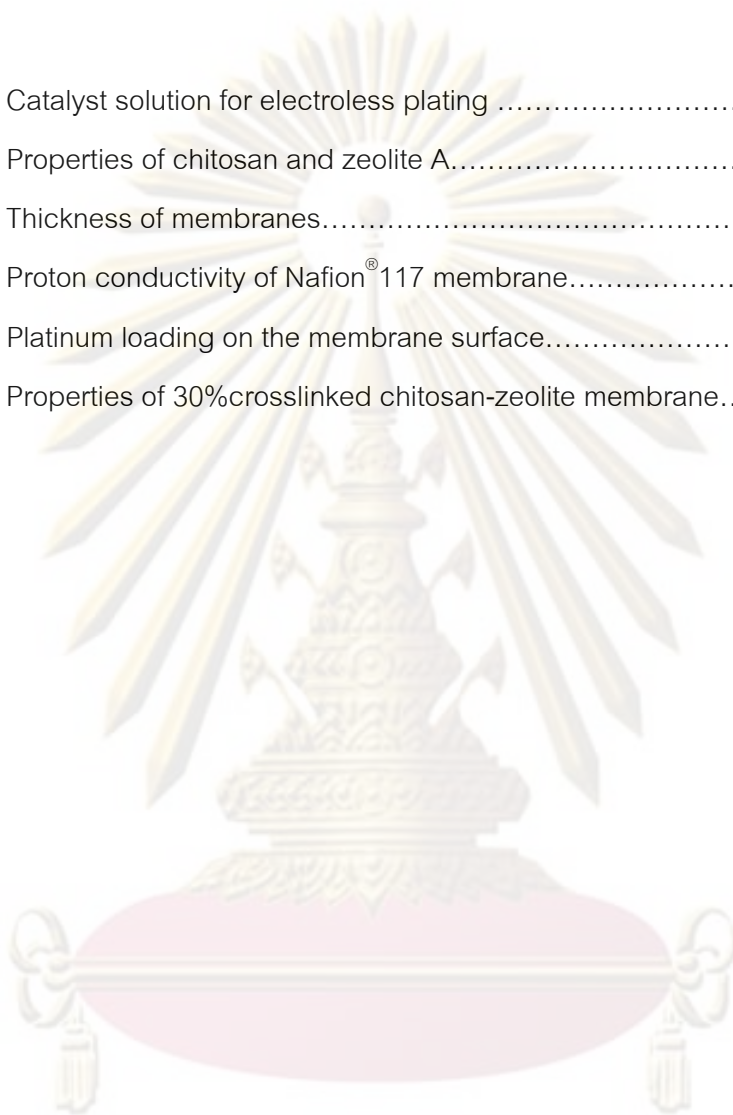
	Page
4.1 Basic properties of materials and membranes.....	40
4.2 Tensile strength.....	41
4.3 Ion exchange capability.....	42
4.4 Gas permeability.....	43
4.5 Membrane Proton Conductivity.....	46
4.6 Platinum Plated Chitosan Based Membranes.....	50
4.6.1 Morphology and Platinum Loading.....	51
4.6.2 Proton Conductivity of Platinum-plated Membrane.....	52
4.6.3 H ₂ Permeability.....	56
4.7 Proton Conductivity in a Single Cell.....	56
4.8 Effect of Relative Humidity on the Fuel Cell Performance.....	59
CHAPTER V CONCLUSION.....	67
5.1 Conclusion.....	67
5.2 Future direction.....	68
REFERENCES.....	70
APPENDICES.....	74
APPENDIX A.....	75
APPENDIX B.....	93
VITAE.....	97



 ศูนย์วิจัยทรัพยากร
 จุฬาลงกรณ์มหาวิทยาลัย

LIST OF TABLES

Table		Page
3.1	Catalyst solution for electroless plating	36
4.1	Properties of chitosan and zeolite A.....	40
4.2	Thickness of membranes.....	41
4.3	Proton conductivity of Nafion [®] 117 membrane.....	48
4.4	Platinum loading on the membrane surface.....	52
5.1	Properties of 30%crosslinked chitosan-zeolite membrane.....	69



ศูนย์วิทยทรัพยากร
จุฬาลงกรณ์มหาวิทยาลัย

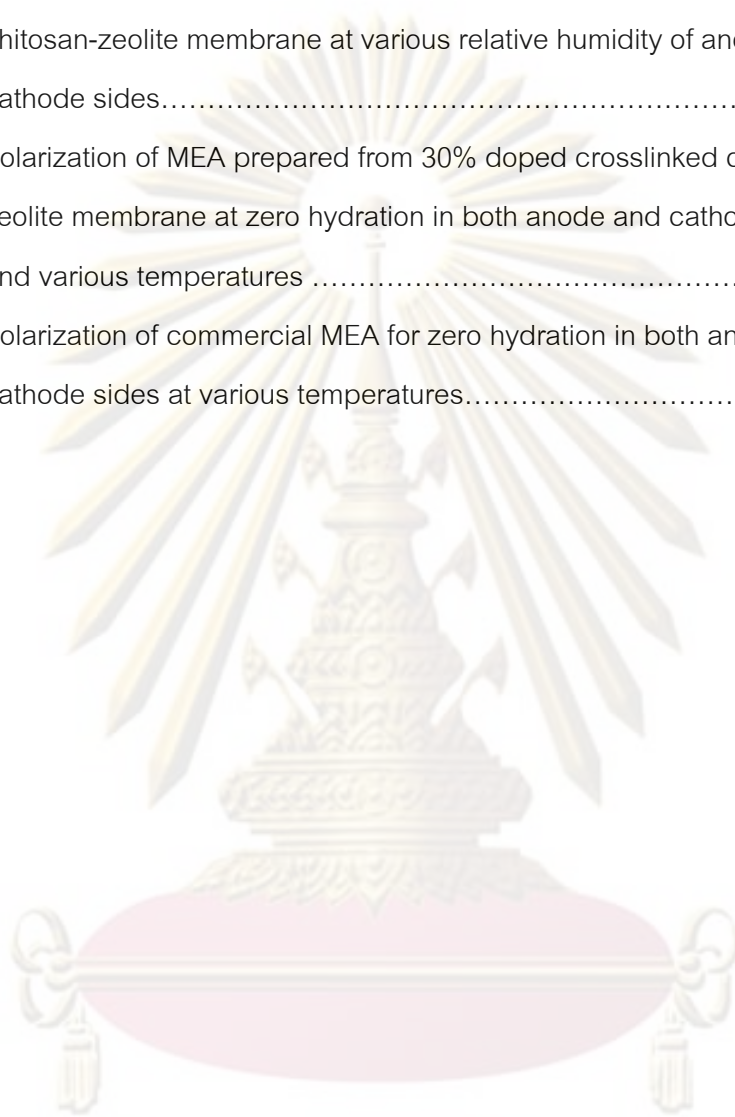
LIST OF FIGURES

Figure		Page
2.1	Schematic diagram of alkaline fuel cell.....	4
2.2	Schematic diagram of molten carbonate fuel cell.....	5
2.3	Schematic diagram of solid oxide fuel cell.....	6
2.4	Schematic diagram of phosphoric acid fuel cell.....	7
2.5	Schematic diagram of direct methanol fuel cell.....	8
2.6	Schematic diagram of PEMFC.....	10
2.7	Chemical structure of PTFE.....	11
2.8	Chemical structure of sulfonated PTFE.....	12
2.9	PEMFC with absorbed water molecules.....	12
2.10	Components of proton exchange membrane fuel cell.....	14
2.11	Chemical structure of chitosan	14
2.12	Morphology of Zeolite A.....	16
2.13	Crystal structure of Zeolite A observed by SEM.....	17
2.14	Production of water in PEMFC.....	22
2.15	Polarization of PEMFC.....	24
3.1	Fuel cell test station.....	30
3.2	Universal testing LLOYD instruments LR 5K.....	33
3.3	Gas permeability test unit.....	34
3.4	Schematic diagram of proton conductivity measurement by four probes technique.....	36
3.5	Teflon mold for electroless plating	37
3.6	Single fuel cell unit.....	38
3.7	A fuel cell test station.....	39
4.1	Tensile strength of crosslinked chitosan-zeolite membrane and sulfuric acid doped crosslinked membrane	42

Figure	Page
4.2 Ion exchange capacity of crosslinked chitosan membrane.....	43
4.3 H ₂ permeability of crosslinked and uncrosslinked chitosan-zeolite composite membranes at various temperatures.....	44
4.4 Effect of sulfuric acid doping on H ₂ permeability of crosslinked chitosan-zeolite membrane at various temperature.....	45
4.5 H ₂ permeability of 30% crosslinked chitosan-zeolite composite membrane at various conditions.....	46
4.6 Proton conductivity of uncrosslinked and crosslinked chitosan-zeolite composite membrane at room temperature (30°C).....	47
4.7 Proton conductivity of crosslinked chitosan-zeolite membrane and Nafion membrane at various temperatures.....	48
4.8 Proton conductivity at 30°C of doped and undoped crosslinked chitosan-zeolite membrane.....	49
4.9 Comparison of membrane conductivity measured by four probes method feeding with nitrogen gas and hydrogen gas of various membranes and temperatures.....	50
4.10 Surface morphology of 30% crosslinked chitosan-zeolite composite membrane at a magnification of 3,000.....	51
4.11 EDX spectrum of 30% crosslinked chitosan-zeolite composite membrane after electroless plating at 60°C for 90 minutes.....	52
4.12 Membrane proton conductivity of platinum-plated crosslinked chitosan-zeolite membrane at various temperatures.....	53
4.13 Comparison of membrane proton conductivity at 30% zeolite contents in various membrane types and temperatures after plating at 60°C for 90 minutes	54
4.14 Electron conductivity of unplated and plated membranes in nitrogen atmosphere at various temperatures	55

Figure	Page
4.15 Comparison in H ₂ permeability at various conditions and temperatures of plated and unplated 30% crosslinked chitosan-zeolite membrane...	56
4.16 Cross sectional proton conductivity of 30% zeolite contents MEA in fuel cell at various membrane types and temperatures.....	58
4.17 Comparison of proton conductivity in planar view and of MEA in fuel cell of doped crosslinked chitosan-zeolite membrane at various temperatures.....	59
4.18 Polarization at 30°C of MEA prepared from 30% uncrosslinked chitosan-zeolite membrane at various relative humidity of anode and cathode sides.....	60
4.19 Polarization at 30°C of MEA prepared from 30% crosslinked chitosan-zeolite membrane at various relative humidity of anode and cathode sides.....	60
4.20 Polarization at 30°C of MEA prepared from 30% doped crosslinked chitosan-zeolite membrane at various relative humidity of anode and cathode sides.....	61
4.21 Polarization at 30°C of MEA prepared from 30% zeolite contents of uncrosslinked, crosslinked and doped crosslinked chitosan membrane at zero hydration in both anode and cathode sides.....	61
4.22 Polarization at 30°C of commercial MEA at various relative humidity of anode and cathode sides.....	62
4.23 Polarization at 30°C of MEA prepared from doped crosslinked chitosan-zeolite membrane for zero hydration in both anode and cathode sides.....	63
4.24 Polarization at 60°C of MEA prepared from 30% doped crosslinked chitosan-zeolite membrane at various relative humidity of anode and cathode sides.....	64

Figure		Page
4.25	Polarization at 90°C of MEA prepared from 30% doped crosslinked chitosan-zeolite membrane at various relative humidity of anode and cathode sides.....	64
4.26	Polarization of MEA prepared from 30% doped crosslinked chitosan-zeolite membrane at zero hydration in both anode and cathode sides and various temperatures	65
4.27	Polarization of commercial MEA for zero hydration in both anode and cathode sides at various temperatures.....	65



ศูนย์วิทยทรัพยากร
จุฬาลงกรณ์มหาวิทยาลัย

CHAPTER I

INTRODUCTION

1.1 Statement of Problem

The high demand in energy causes fossil fuels to rapidly decrease. Another form of environmental friendly alternative energy is developed by researchers worldwide. The proton exchange membrane fuel cell (PEMFC) is of interest in this study. Chitosan-zeolite composite membranes have been characterized a potential candidate for substitution of commercial Nafion membrane [1-3]. In previous study [4-5], platinum (Pt) and palladium (Pd) have been applied successfully as catalyst layers on chitosan membranes directly by electroless plating technique for preparing the membrane electrode assembly (MEA) component.

The performance of PEMFC depends on the membrane properties as well as the operating condition especially the relative humidity in the MEA. It is believed that the proton could move through the membrane from anode to cathode in the form of hydronium ion (H_3O^+). In order to decrease the CO poison on Pt catalyst, fuel cells are usually operated at high temperature resulting in the membrane dehydration and low performance.

The high hydrophilicity of chitosan-zeolite composite membranes may have a benefit for PEMFC on high temperature operation and omitting external humidifier. However, this must be clarified.

1.2 Objective

This research is aimed to study the effect of humidity on FC performance of chitosan-zeolite composite membranes.

1.3 Scope of investigation

1. The studied membranes were uncrosslinked chitosan, uncrosslinked chitosan-zeolite, crosslinked chitosan, crosslinked chitosan-zeolite, doped crosslinked chitosan, and doped crosslinked chitosan-zeolite membrane.
2. Zeolite A was incorporated in the range of 10-30% by weight of chitosan.
3. Membranes were characterized for
 - 3.1 Tensile strength
 - 3.2 Ion exchange capability
 - 3.3 Hydrogen permeability at 30, 60, and 90°C
 - 3.4 Proton conductivity in planar view at 30, 60, and 90°C
4. The Pt catalyst layer was coated on membrane by electroless plating technique following the previous study [5] and characterized for
 - 4.1 Membrane morphology and the platinum quantity by using Scanning Electron Microscope/Energy Dispersive Spectrometer
 - 4.2 Hydrogen permeability at 30, 60, and 90°C
 - 4.3 Proton conductivity in planar view at 30, 60, and 90°C
5. The plated membranes was sandwiched between teflon-treated carbon papers from Electro Chem. Inc. and pressed by the compression mold at 37-40°C and 30 kg/cm² for 1 minute as membrane electrode assembly (MEA) and characterized for
 - 5.1 Proton conductivity in cross section view at 30, 60, and 90°C
 - 5.2 Cell performance at 30, 60, and 90°C and various relative humidity

CHAPTER II

THEORY AND LITERATURE REVIEW

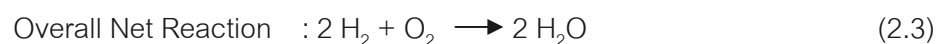
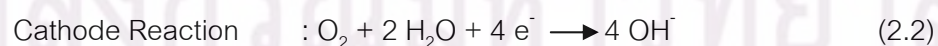
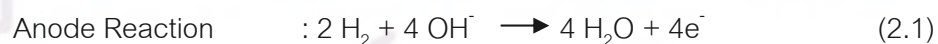
2.1 Fuel cell technology [1]

Fuel cell is a device or instrument which convert chemical power from the fuel into electricity (direct current). Fuel cell is consisted of porous electrodes (anode and cathode) immersed in electrolyte which can be in either liquid or solid form. Fuel can be natural gas or hydrogen gas which is fed into anode where oxidation takes place and then electron will be released while oxidant will be transferred to cathode where reduction takes place resulting in direct-current (DC). Electrodes act as reaction sites for the electrochemical and redox reactions of fuel cells. Fuel cell can be classified based on types of electrolytes into 6 categories as follows:

2.1.1 Alkaline Fuel Cells (AFC) [6]

Alkaline fuel cell utilizes 30-43 weight % of potassium solution as electrolyte. This fuel cell is appropriate for room temperature and yields the highest potential difference at the same current densities when compared with other types of fuel cells.

Alkaline fuel cell works by feeding high purity fuel that does not contain CO₂ into the anode. The oxidation takes place as shown in equation 2.1 and oxygen is fed into cathode as shown in equation 2.2.



The schematic diagram of alkaline fuel cell is shown in figure 2.1. The power production efficiency is as high as 70% and the life time of 10,000 - 15,000 hours. The disadvantage of this fuel cell is that high purity hydrogen gas is required since CO_2 can produce CO_3^{2-} in electrolyte which is basic resulting in clogging. Therefore, CO_2 removal has to be conducted which is an expensive task.

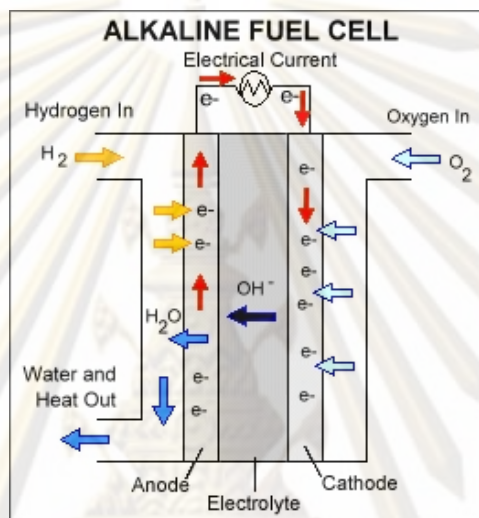
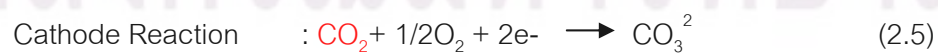
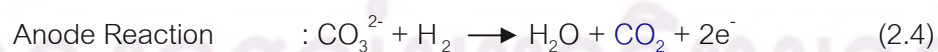
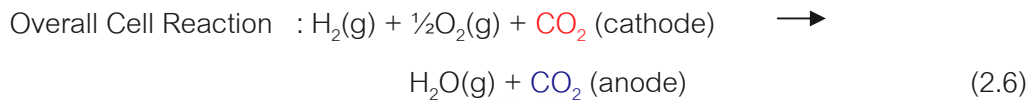


Figure 2.1 Schematic diagram of alkaline fuel cell [7]

2.1.2 Molten Carbonate Fuel Cells (MCFC) [8]

Molten carbonate fuel cell uses a mixture of Li_2CO_3 and K_2CO_3 on LiAlO_2 as an electrolyte. CO_2 is flowed from anode to cathode as shown in equation 2.4 and 2.5. The temperature of working fuel cell is in the range of 500 - 700 ° C. Since the operating temperature is high; therefore, Pt is not required as a catalyst for the electrodes.





The schematic diagram of molten carbonate fuel cell is shown in figure 2.2. Different types of fuel such as H₂, CO, natural gas, methane, and gas obtained from coal gasification, etc. can be used. However, H₂S contamination in the fuel needs to be considered since this gas is toxic to the electrodes. The working temperature of this fuel cell is approximately 650 °C and the electrical power generated is in the range of 10 kW – 20 MW.

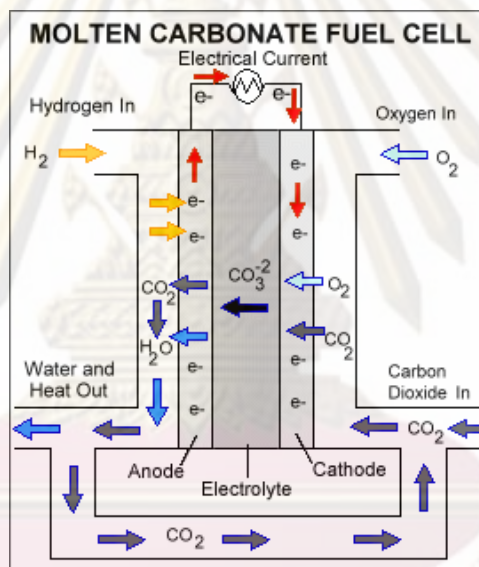


Figure 2.2 Schematic diagram of molten carbonate fuel cell [9]

2.1.3 Solid Oxide Fuel Cells (SOFC) [10]

Solid oxide fuel cells utilize electrodes and electrolyte fabricated from ceramic or solid oxide such as yttria and zirconia. These material can conduct O²⁻ ion at the temperature higher than 800 °C. The working temperature is approximately 1,800 °F or 1,000 °C. At this high temperature, fuel such as natural gas and liquid fuel can be converted to H₂ for the reaction at the anode as shown in equation 2.7. The schematic

diagram of solid oxide fuel cell is illustrated in figure 2.3. The electrical power generated is as high as 100 kW.

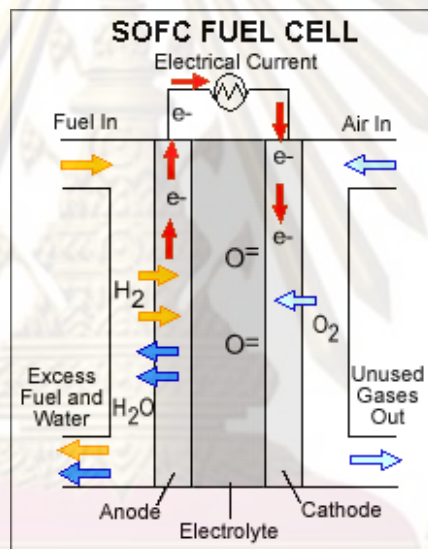
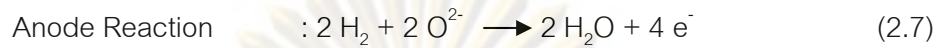
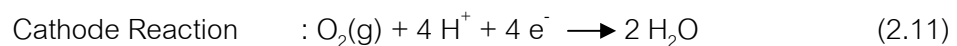
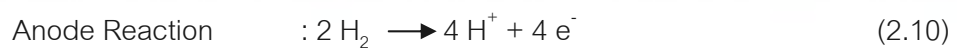


Figure 2.3 Schematic diagram of solid oxide fuel cell [11]

2.1.4 Phosphoric Acid Fuel Cells (PAFC) [12]

Phosphoric acid fuel cells use phosphoric acid as an electrolyte where it was stored in silicon carbide matrix. The electrochemical reaction takes place in an acid media as shown in equation 2.10 and 2.11:





The working temperature is in the range of 170 – 200 °C. High temperature helps stabilize phosphoric electrolyte and reduces the toxic from CO₂ which diminishes the catalyst efficiency. The schematic diagram of phosphoric acid fuel cells is shown in Figure 2.4. The life time is as long as 40,000 hours. The power generated is as high as 40%. Moreover, it can produce 85% of water vapor when operating at high temperature. At present, the capacity of this fuel cell is around 1kW and 1 MW.

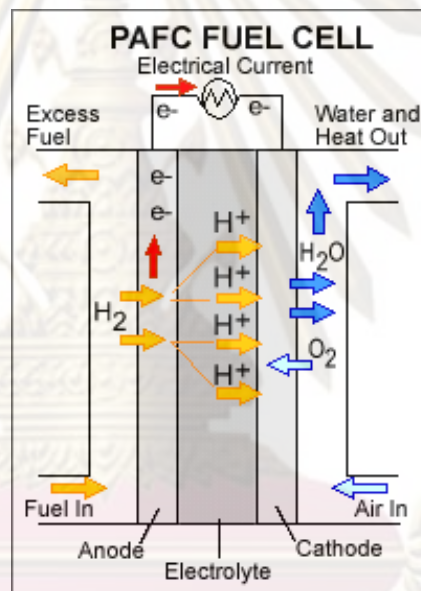
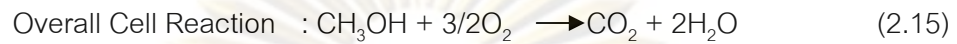
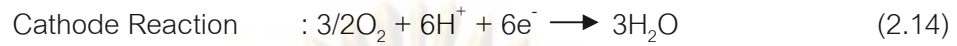
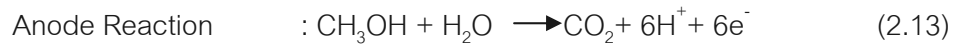


Figure 2.4 Schematic diagram of phosphoric acid fuel cell [13]

2.1.5 Direct Methanol Fuel Cells (DMFC) [14]

Direct methanol fuel cell was developed from proton exchange membrane fuel cell. This fuel cell can produce electricity directly from methanol without having to pass through the reformer. The schematic diagram of direct methanol fuel cell is shown in figure 2.5. Methanol is fed directly in to anode while O₂ is fed into cathode as shown in equation 2.13 and 2.14:



The efficiency of this type of fuel cell is approximately 40% at a working temperature range 50 - 100 °C. Since it can be used at low temperature, direct methanol fuel cell is appropriate for the energy source of mobile electronics such as laptop, mobile phone, etc. Moreover, it is also suitable for electrical cars that use methanol as fuel.

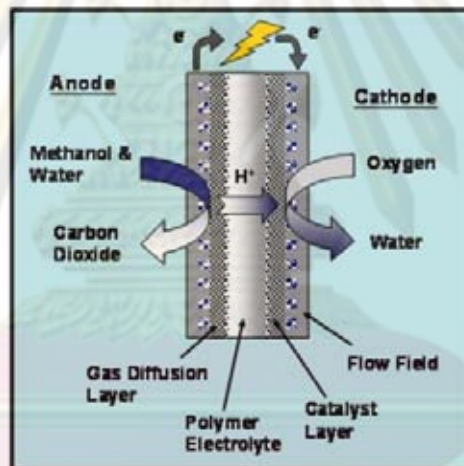
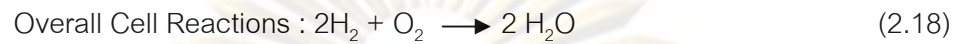
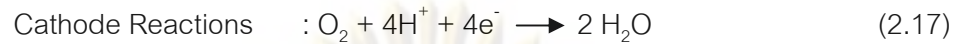
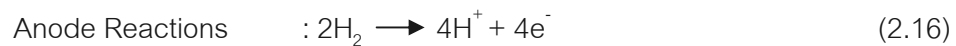


Figure 2.5 Schematic diagram of direct methanol fuel cell [14]

2.1.6 Proton Exchange Membrane Fuel Cells (PEMFC) [15]

Proton exchange membrane fuel cell uses proton exchange membrane as an electrolyte. The reaction taking place at the electrodes is similar to that of phosphoric acid fuel cell as shown in equation 2.16 and 2.17. The exchange membranes are sandwiched between the electrodes which are made of carbon with Pt coated on the surface as shown in figure 2.6



This working temperature of this fuel cell is approximately 175 °F or 80 °C which can generate power in the range of 50-250 kW. Since this fuel cell can be operated at moderate temperature range and give high electrical power, many researchers have been working to further improve the performance of this type of fuel cell which will be discussed later.

2.2 Principle of proton exchange membrane fuel cell (PEMFC)

PEMFC is consisted of porous cathode and anode immersed in electrolyte which can be in either solid or liquid form. Fuel can be natural gas or hydrogen gas which is fed into anode where oxidation takes place and then electron will be released while oxidant will be transferred to cathode where reduction takes place resulting in direct-current (DC). Electrodes act as reaction sites for the electrochemical and redox reactions of fuel cell (Figure 2.6). In case where the high potential difference is required, several fuel cells have to be combined. [16]

ศูนย์วิทยทรัพยากร
จุฬาลงกรณ์มหาวิทยาลัย

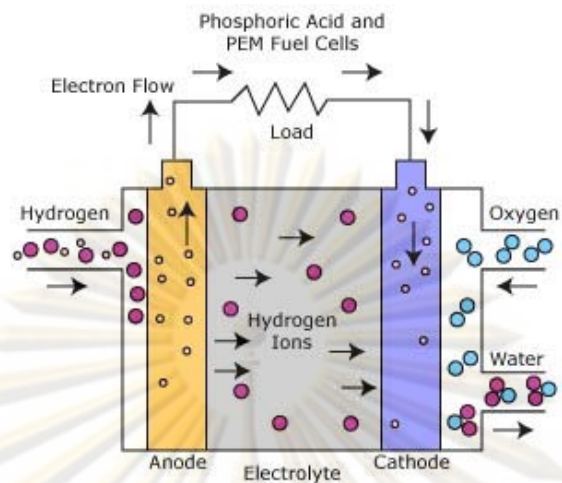


Figure 2.6 Schematic diagram of PEMFC [15]

2.3 Components of proton exchange membrane fuel cell [17]

PEMFC system contains the following:

2.3.1 Current Collector Plate [17]

The current collector plate is placed between each fuel cell. It can be classified into two types: unipolar plate and bipolar plate. These plates are made from a variety of materials including graphite, polymer alloys, metals, etc.

2.3.2 Membrane Electrode Assembly (MEA) [17]

Membrane electrode assembly is a proton exchange media which consists of a membrane sandwiched between two porous electrodes that have Pt coated on the surface.

The requirements of membrane electrode assembly are:

- Electrode

The electrodes consist of anode where the oxidation takes place giving positive ion and electrons, and cathode which receive positive ion that passed through proton exchange membrane. Electrodes should have good electrical conductivity, high porosity and large surface area to increase the reactive sites. The electrodes should be contacted directly to the electrolyte in order to decrease the internal resistance. Porous carbon is usually used as the electrodes since it has great electrical conductivity and high melting temperature. However, porous carbon has to be coated with Teflon in order to improve hydrophobicity in order to prevent the cell flooding.

- Electrolyte

Commercial proton exchange membrane such as Nafion is usually made of polymer that contains mainly sulfonated groups or fluoroethylene. The membrane was usually prepared through perfluorination yielding tetrafluoroethylene. After polymerization, Polytetrafluoroethylene or PTFE is obtained. The chemical structure of PTFE is shown in figure 2.7. The chemical bonds between fluorine and carbon in Nafion are very strong yielding membranes with great mechanical strength.

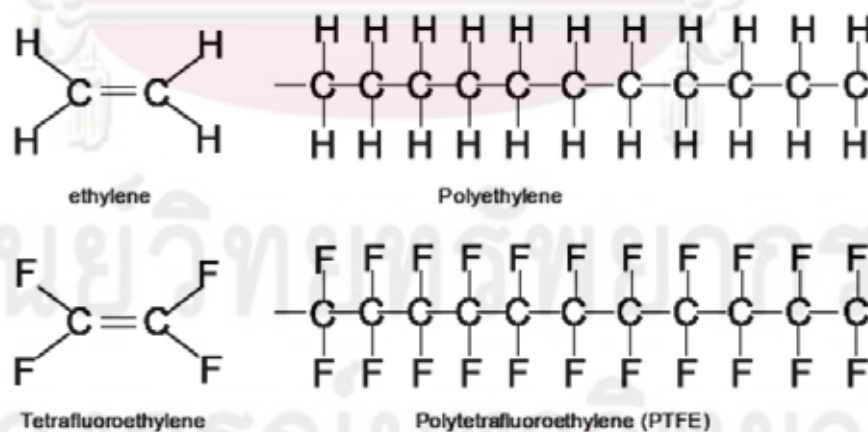


Figure 2.7 Chemical structure of PTFE [18]

Sulfonate is added into PTFE by using sulfonic acid as shown in figure 2.8. Sulfonic acid reacts at the end of PTFE chain forming SO_3^{2-} groups which are hydrophilic.

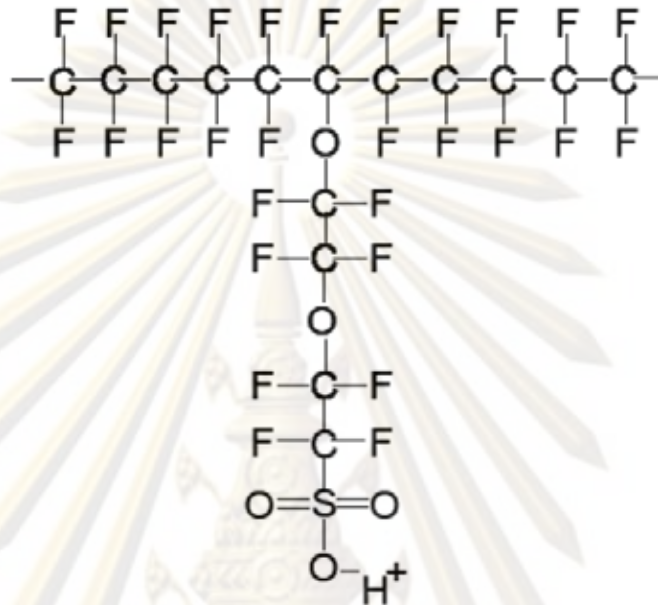


Figure 2.8 Chemical structure of sulfonated PTFE [18]

Hydrophilic regions adsorb water into the electrolytes as shown in figure 2.9 which weakening the bonds between SO_3^{2-} and H^+ ; therefore, H^+ can move easily.

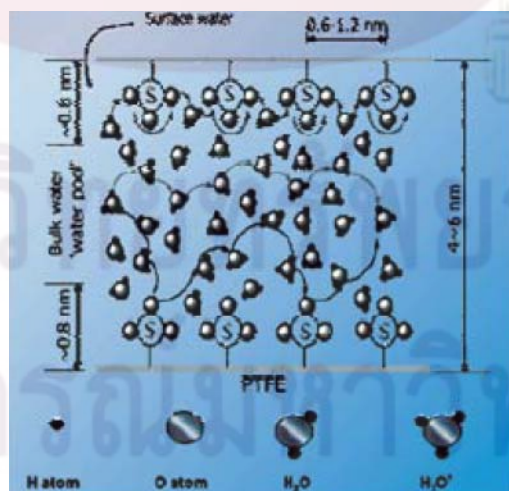


Figure 2.9 PEMFC with absorbed water molecules [18]

The requirements of proton exchange membranes are [1]:

- 1) Good proton conductivity but low electron conductivity
- 2) Low gas permeability
- 3) Good dimensional stability
- 4) Excellent mechanical properties
- 5) Low water diffusion
- 6) Low resistance for losing water.
- 7) Good resistance to oxidation, reduction and hydrolysis
- 8) Good cationic exchange capability
- 9) Electrode surface can be easily coated with catalyst
- 10) Homogeneity

- Catalyst

Precious metals such as Pt and Pd are usually used as catalysts. Pt is the most widely used catalyst for PEMFC since it has good chemical resistance yielding the electrodes that have good stability and great electrochemical reactivity when compared with other metals. Components of proton exchange membrane fuel cell are shown in figure 2.10.

ศูนย์วิทยทรัพยากร
จุฬาลงกรณ์มหาวิทยาลัย

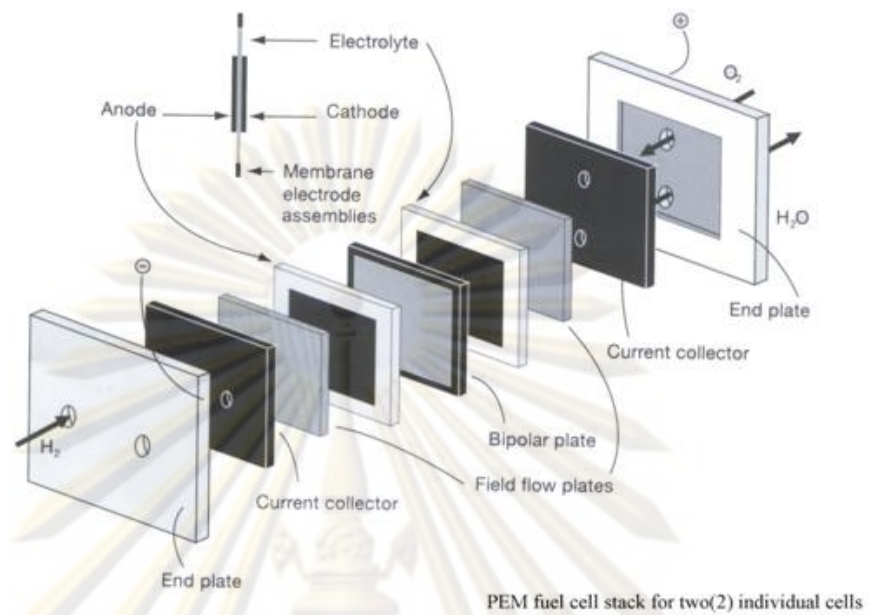


Figure 2.10 Components of proton exchange membrane fuel cell [19]

2.4 Chitin and Chitosan [20]

Chitosan is an insoluble derivative of chitin which can be extracted from shrimp and prawn shells [21]. The chemical nomenclature of chitosan is Poly- β -(1,4)-2-amino-2-deoxy-D-glucose and the formula is $C_8H_{11}O_4N$. The chemical structure of chitosan is shown in figure 2.11.

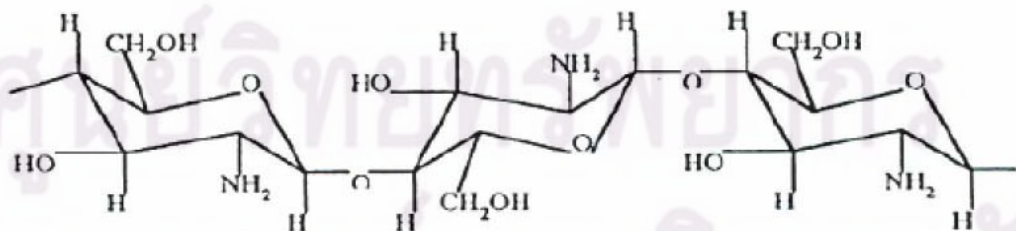


Figure 2.11 Chemical structure of chitosan [21]

Chitosan is obtained through deacetylation of chitin in which single molecule of chitin (N-acetyl glucosamine) is converted into glucosamine. Deacetylation enables chitosan to be very active and can react with secondary amine and secondary alcohol [22]. Chitosan is categorized as polycation. When 50% of chitin was deacetylated, the obtained product is chitosan.

Chitin is not soluble in water, dilute acid, dilute base, concentrated alcohol or solvent but will be soluble in concentrated hydrochloric, sulfuric, phosphoric or formic acids. Solubility depends on molecular densities and different functional groups.

Chitosan is not soluble in water, base or organic solvent but can be dissolved in all organic acid. Acetic and formic acids are generally used. Some inorganic acids such as nitric, hydrochloric, perchloric and phosphoric acid can also be used if the mixtures are stirred at moderate temperature. Chitosan which is a viscous clear liquid shows non-newtonian behavior. The viscosity of chitosan depends on several factors such as % deacetylation, molecular weight, ionic strength, pH, and temperature. The viscosity is generally decreased when the temperature is increased.

2.5 Zeolite [23]

Zeolite is a crystallite aluminosilicate. The unit cell of zeolite contains Si or Al and 4 atoms of oxygen (SiO_4 or AlO_4) bonded in a tetrahedron shape. Si or Al is located in the centered surrounded by oxygen atom in all four corners. Oxygen is shared between each molecule resulting a larger structure with pores in the molecules. Zeolite can range from 2-10 angstrom. Some positive ions such as Na^+ , K^+ , or Ca^{2+} are loosely packed inside the zeolite cage. Water is also absorbed in zeolite molecules. The general formula structure of zeolite is shown in equation 2.19.



where n is valence of cation (M) usually equals to 1 or 2

x is mole of SiO_4 (generally ≥ 2)

y is mole of water in zeolite pores

Morphology of zeolite A as shown in figure 2.12. Crystal structure of zeolite A was observed by SEM as shown in figure 2.13. The pore volume of zeolite A is $0.47 \text{ cm}^3/\text{g}$. The diameter of the pore is 4.2 angstrom.

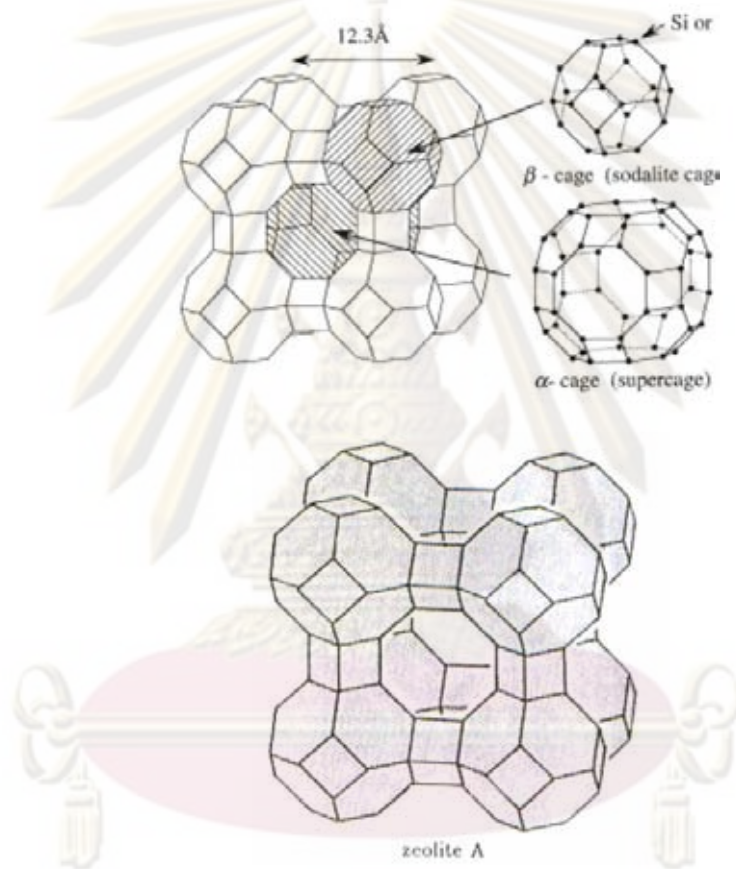


Figure 2.12 Morphology of Zeolite A [22]

ศูนย์วิจัยทรัพยากร
จุฬาลงกรณ์มหาวิทยาลัย

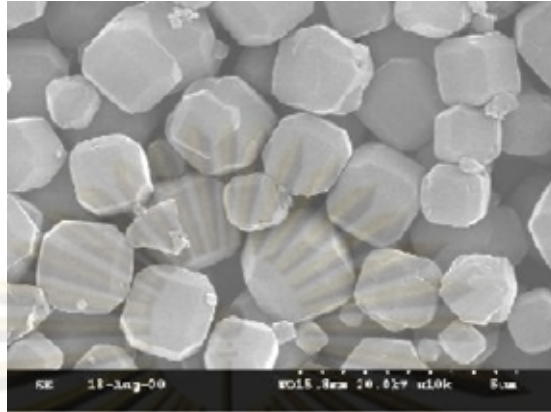


Figure 2.13 Crystal structure of Zeolite A observed by SEM [24]

2.6 Preparation of Membrane electrode assembly (MEA) [25]

The catalyst solution can be loaded either on gas diffusion layer or on membrane by spraying, painting or electrochemical reaction. In this study, the electroless deposition is selected on the preparation method for MEA.

2.6.1 Gas diffusion layer/Catalyst assembly [25]

Gas diffusion layer/ catalyst assembly can be prepared by different methods as follows:

- Spraying

Homogeneous catalyst mixture is sprayed on porous carbon. The viscosity of the mixture has to be adjusted accordingly while the appropriate drying time also needs to be considered. The mixture should have low viscosity for good dispersion of the catalyst on the carbon electrodes.

Painting

Painting is used with a higher viscosity mixture. The mixture is painted on the support such as carbon paper or cloth. The support can be used as electrodes in order to enhance the permeability and maintain the humidity in the fuel cell.

- Electroless deposition

Electro deposition is conducted through the electrochemical reaction on carbon paper which is immersed in the catalyst solution where the electricity is applied to. After that, carbon paper is rinsed with distilled water to remove remaining metal and dried.

2.6.2 Membrane/Catalyst assembly [25]

Membrane/catalyst assembly can be prepared as follows:

- Spraying

The catalyst solution is directly sprayed onto the membranes before hot pressing.

- Painting

This method is similar to the one discussed earlier. However, when thin membrane and high concentration mixture are used, the dispersion might be poor resulting in the increase of the internal resistance. Moreover, drying temperature should be low to prevent cracking.

- Electroless deposition

Electroless deposition is carried out through chemical reaction of metal ions in the solution containing reducing agent. This method is used in this study and will be further discussed.

2.7 Electroless deposition [5]

The catalyst layer is formed on the surface of the substrate through electrochemical reaction of reducing agent and metal ions in solution. The surface of the substrate should have good catalytic surface.

The reactivity of the autocatalytic reaction depends on amount of metal ions in solution and the catalytic surface. The reduction is autocatalytic and quite complicate. The intermediate products obtained from this reaction can be hydrogen atom, hydrogen ion, or hydrogenated compound. The reducing agent is anodically oxidized yielding electrons on the catalytic surface. The metal ions will receive the electrons resulting in cathodically reduced reaction as shown in equation 2.20 and 2.21. Both reactions take place almost simultaneously and electrons are the active intermediate products.

Oxidation takes place on the reducing surface of the substrate:



Reduction of metal ions:



The electroless deposition process can be varied yielding different intermediates which can be hydrogenated compounds that are very reactive or compounds with water causing precipitation of metal oxide prior to reduction. Several parameters affecting the reaction rate and coating efficiency have to be considered.

- Solution mixtures for electroless deposition

The important ingredients are metal ions and appropriate reducing agent. The metal should be stable, water soluble, and easily reduced. It can be in the form of complex ions or ion salts. The general metal used for this process are Cu, Ni, Au, Ag, Pd

or Pt, etc. Some chemicals such as complexing agent, stabilizer, pH buffer and brightener are sometimes added.

- Reducing agent

Reduction of metal ions in solution requires strong specific reducing agent which has good electron conductivity, non-toxic, and no release of toxic gas. The amount of reducing agent used depends on types of metal and reaction.

Most reducing agent used in electroless deposition contains hydrogen such as hydrogen with phosphorus, nitrogen, or carbon. Some catalyst such as Ni or Pd are sometimes used. Autolytic reaction can be obtained through appropriate selection of reducing agent. Some reducing agent such as BH_4^- can be used with a variety of metals. The efficiency also depends on pH of the solution in which the reducing agent can be appropriate dissolved without precipitation.

- Stability of plating solution

The solution contains metal ions, reducing agent, additives. The solution stability decrease when the concentration and temperature are increased resulting in metal precipitation and reduced thickness. In order to increase the stability, the starting concentration should be suitable. The additives such as stabilizer should be added. Two types of additives are available. The first is the inhibitor such as sulfur or cyanide compounds. Another type is electron acceptor where approximately 1-100 mg/l is appropriate. In some cases, Stabilizer can increase the reaction rate; however, the concentration should be adjusted accordingly.

The advantages of electroless deposition are:

1. No electrical current is required
2. Metal can be coated on an insulating or semi-conducting substrate if they are stable in the solution. The surface should be prepared for this process.
3. The metal layer should be homogenous. The thickness of this metal layer depends on the compositions of the solution.

4. Strong adhesion between the substrate and the coating metal
5. Not complicate and can be directly applied on the substrate.
6. The solutions can be adjusted to increase the efficiency.

The disadvantages of electroless deposition are the appropriate selection of reducing agent, slow reaction rate and difficult to control.

2.8 Effects of parameters on the performance of PEMFC [26]

The effects of parameters on the performance of fuel cells will be studied as follows:

2.8.1 Effect of water on the performance of PEMFC [26]

The performance of fuel cell depends on hydrogen exchange capability which require water in the system. The performance decreased when the amount of water is low. However, too much water can cause cell flooding.

Generally, hydrogen ion is carried by 1-2.5 water molecule [27]. This process is called electro-osmotic drag. When high voltage is applied, this process can cause dryness on the anode. When air is used as an oxidizing agent at the temperature higher than 60°C, air will case the electrode to dry faster than the water being generated from cathode [26]. In order to solve this problem, air and oxygen are humidified before passing into fuel cell. However, this method is complicated, increase the weight and more expensive [28]. Therefore, choosing the membrane that can absorb water can reduce this problem.

Figure 2.14 shows how water is produced in PEMFC. On the right corner of this figure, water is produced on the cathode. The water permeability between cathode and anode depends on the thickness of proton exchange membrane and equilibrium humidity on both electrodes. Humidifier will reduce this problem.

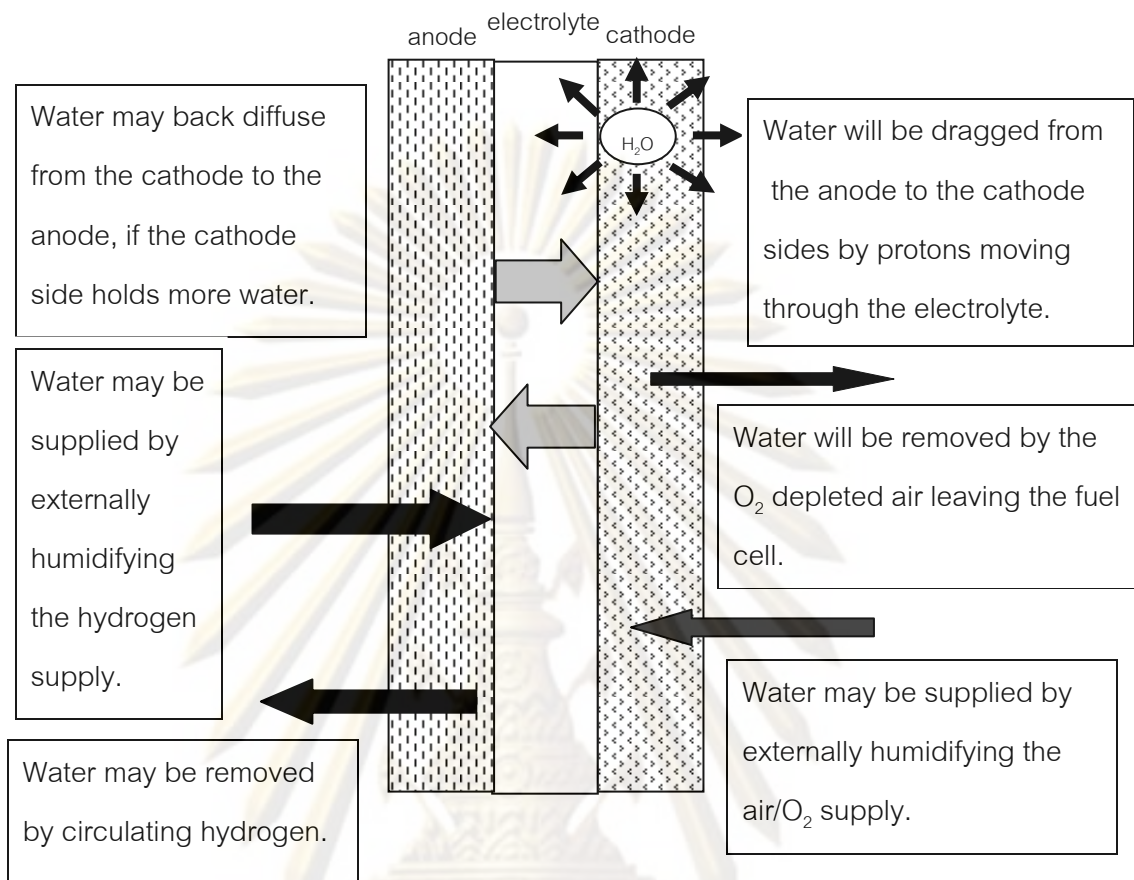


Figure 2.14 Production of water in PEMFC [26]

2.8.2 Effect of temperature on PEMFC performance [29]

When temperature is increased, chemical polarization is decreased and the rate of reaction increased resulting in better performance. However, if the temperature is too high, the potential difference will be decreased drastically causing possible dehydration of proton exchange membrane and higher internal resistance unless humidifier is applied in the system or membrane used has good water absorbability.

2.9 Polarization [30]

When fuel cell is completely connected, the electrical current will be distributed to the appliances. However, the reduction of the potential difference of fuel cell is not equal to that of theoretical or from reversible process. The difference in the potential difference, so called polarization, can be occurred on both cathode and anode causing reduced potential difference. The real potential of the fuel cell (E_{cell}) can be calculated from the following equation:

$$E_{\text{cell}} = E_{\text{cell}}^{\circ} - |\xi_{\text{c}}| - |\xi_{\text{a}}| - IR \quad (2.22)$$

where E_{cell}° is the standard potential when compared with standard hydrogen electrode

ξ_{c} is over potential at cathode

ξ_{a} is over potential at anode

IR is over potential caused by internal resistance in fuel cell

The plot between potential difference and current density is shown in figure 2.15.

ศูนย์วิทยทรัพยากร
จุฬาลงกรณ์มหาวิทยาลัย

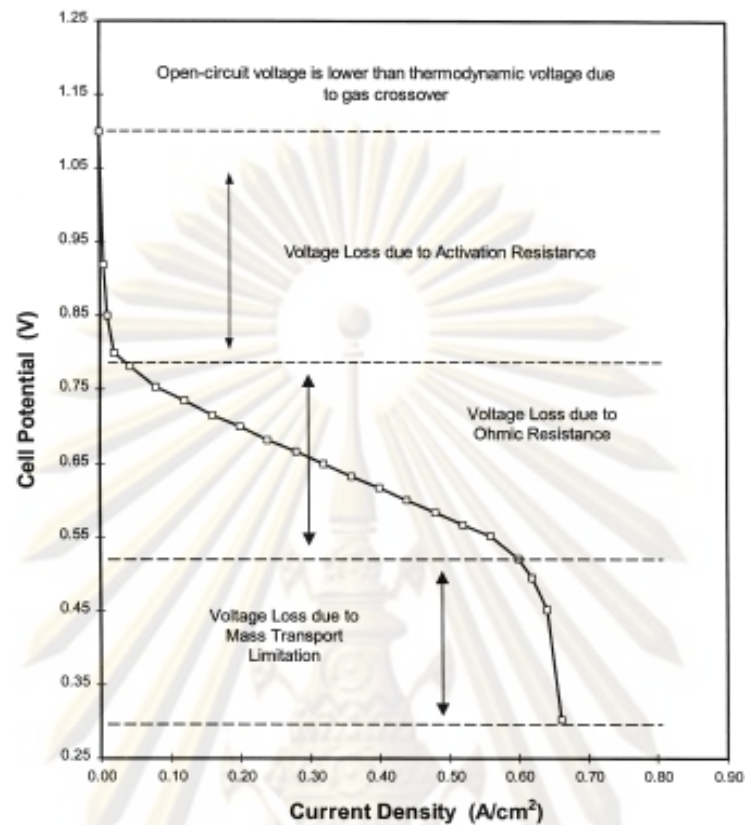


Figure 2.15 Polarization of PEMFC [31]

From figure 2.15, at the current density equals to zero, the obtained potential difference was less than that of the theoretical value. This potential is called open-circuit potential which caused by gas cross over between cathode and anode through proton exchange membrane. When gas crossed over from cathode, oxidation took place while at cathode, oxygen caused reduction at the same cathode resulting in internal current and over potential at cathode [26]. At anode, oxygen crossed over causing over potential at anode resulting in reducing potential difference.

Three types of polarization can take place including Chemical Polarization, Resistance Polarization and Concentration Polarization.

2.9.1 Activation Polarization or Chemical Polarization [32]

This process is caused by chemical reaction and physical chemistry of the molecules absorbed on the electrodes similar to activation energy in which the rate of reaction is controlled. The reaction takes place only when the energy generated from the reaction is higher than the activation energy. If the potential energy is high, the rate of reaction is low causing high chemical polarization. This problem can be solved by increasing the energy of the reactants such as increasing temperature [33]. However, this method is inappropriate for PEMFC since proton exchange membrane cannot be operated at high temperature. The appropriate method to reduce the potential activation energy is to use an effective catalyst [34].

2.9.2 Resistance polarization [26]

This type of polarization cause by the resistance of the electron mobility on electrodes and current collector which do not have good electrical conductivity or the resistance of proton mobility from anode to cathode since water is required to carry proton through the membrane.

Over potential is increased according to the resistance of electrolyte in fuel cell which is related to the current density as shown in the following equation:

$$\varepsilon_R = jAR \quad (2.23)$$

where A is the surface area of the electrode. Resistance is related to conductivity, k where x is thickness of electrolyte

$$R = \frac{x}{kA} \quad (2.24)$$

Replacing the value obtained from equation 2.24 into equation 2.23:

$$\varepsilon_R = \frac{jx}{K} \quad (2.25)$$

This problem can be solved by using appropriate catalyst and current collector that has good electrical conductivity in order to reduce the electron resistance. Electrolyte layer should be thin in order to decrease the distance of the proton mobility or increasing the humidity of electrolyte by using membrane that can absorb water.

2.9.3 Concentration Polarization [32]

This type of polarization caused by the rapidly decrease of oxidizing agent. Usually, this problem can be avoided by using high purity oxygen gas. When air is used as oxidizing agent, the gas carrier path need to be designed to allow air to contact with the catalyst.

2.10 Humidity [26]

Specific humidity or absolute humidity is the ratio between water vapor mass in air or gas to mass of dried air or gas in one cubic volume.

Relative humidity is the humidity in air or gas in which can be calculated from the ratio of real water vapor in air or gas to mass of saturated water vapor in air or gas in one cubic volume which can be calculated as percent relative humidity.

At the relative humidity equals to 100 water partial pressure is equal to saturated vapour pressure. At this condition, water cannot penetrate into gas resulting in equilibrium state where the evaporating rate is equal to the condensation rate. However, since saturated water vapor pressure depends on temperature, when the temperature increase, the evaporation rate increase higher than the condensation rate. The opposite phenomena takes place when the temperature decreased. [26]

2.11 Related works

Pitsanu (1983) [30] used Pt coated stainless steel electrode and found that the performance was improved when the working temperature was increased. When comparing between thick and thin ion exchange membrane, thinner membrane showed better performance due to less internal resistance.

Unchalee (2003) [2] studied sulfuric acid crosslinked chitosan and composite chitosan membrane with lithium nitrate and lithium acetate by using ethylene carbonate as a plasticizer. They found that the proton conductivity was highest when 50% of lithium nitrate and sulfuric acid was doped on membrane. The ion exchange capability, hydrogen permeability and tensile strength were higher than those of nafion. However, the proton conductivity was still lower.

Wanwara (2004) [35] prepared Pt coated membrane through electroless deposition using hydrazine solution as a reducing agent. However, they found that the prepared membrane showed poorer performance when compared with commercial Nafion membrane

Prapoj (2005) [3] added 10-80 wt. % of zeolite A which had the ratio of silica to alumina equaled to 1:1 into the crosslinked sulfuric acid doped chitosan membrane and found that at 4 wt. % of sulfuric acid and 50 wt. % of zeolite, the tensile strength, hydrogen gas permeability, ion exchange capability, proton conductivity at room temperature was 53.3 ± 0.6 MPa, 187.0 ± 1.4 Barrer, 5.24 ± 0.03 meq/g and $5.1 \times 10^{-2} \pm 0.6 \times 10^{-3}$ Siemen/cm, respectively.

Watanabe and coworkers (1996) [38] prepared fuel cell that did not required external humidifier by adding SiO_2 , TiO_2 and Pt into the membrane. The metal oxides absorbed water resulting in better performance.

Buchi and Srinivasan (1997) [39] studied the effect of temperature and humidity on the performance of the fuel cell. They found that these parameters were crucial to obtain high efficiency.

Andreaus and coworkers (2001) [40] found that when thick membrane was used, the internal resistance was increased while the water permeability from cathode to

anode decreased resulting in cell flooding at cathode. Moreover, water was required to transfer proton in order to reduce the chemical polarization.

Mukoma and coworkers (2004) [36] prepared sulfuric crosslinked chitosan membrane to study the thermal stability, water absorption and proton conductivity for PEMFC. They found that chitosan membrane decomposed at 300 °C and 60 wt.% water absorption which is higher than Nafion that has only 30 wt.% water absorption. When running the fuel cell at 60 °C in a saturated humid condition, Nafion and chitosan membranes showed the proton conductivity equaled to 0.12 and 0.02 Siemen/cm, respectively.

Sun et al. (2005) [37] prepared Pd coated composite Nafion membrane by electroless plating in order to reduce methanol permeability and increase proton conductivity. They found that Pd enhanced proton conductivity of Nafion and increased power generated. However, Nafion can shrink resulting in membrane defect.



ศูนย์วิจัยทรัพยากร
จุฬาลงกรณ์มหาวิทยาลัย

CHAPTER III

EXPERIMENTAL

3.1 Chemicals and Materials

1. Chitosan (commercial grade) from Eland Corporation, Ltd.
2. Zeolite A (Linde type A) (commercial grade) from Thai Silicate, Ltd.
3. H_2SO_4 solution, 98 wt.% (commercial grade)
4. HCl solution, 35 wt.% (AR grade)
5. CH_3COOH solution, 99.5 wt.% (commercial grade)
6. NaOH solution, 50 wt.% (commercial grade)
7. $\text{NH}_3 \cdot \text{H}_2\text{O}$, 28 wt.% (AR grade)
8. $\text{N}_2\text{H}_4 \cdot \text{H}_2\text{O}$, 51 wt.% (AR grade)
9. Na_2EDTA (AR grade)
10. PtCl_2 (purum 60% Pt)
11. H_2 , 99.99% purity from PRAXAIR
12. Air zero from PRAXAIR
13. Teflon treated carbon paper from Electro Chem. Inc., USA
14. Nafion[®] 117 membrane from Electro Chem. Inc., USA
15. Membrane electrode assembly (MEA) from Electro Chem. Inc., USA

3.2 Instruments

1. Ultrasonic water bath, GFL model 1083
2. Mixer with adjustable speed and Teflon blade, IKLABOR TECHNIK model RW 20n
3. Analytical balance, Mettler Toledo model PB 3002-S
4. Hot air oven, Binder model ED 115
5. Glass plates

6. Micrometer
7. Constant pressure gas permeability test unit
8. Four-point probes proton conductivity measurement unit
9. Fuel cell test station at the Department of Chemical Technology, Faculty of Science, Chulalongkorn University as shown in figure 3.1 is consisted of following components

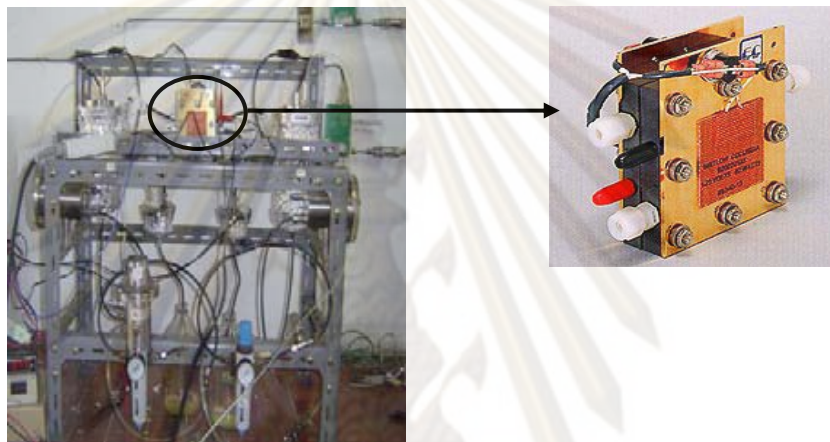


Figure 3.1 Fuel cell test station

- a) 2.3X2.3 cm² Single cell model FC05-01SP-REF from Electro Chem. Inc., USA
- b) Humidifier consisting of evaporation chamber, water supply chamber, and sensor chamber
- c) Temperature controller: model SR17 from Shimaden for controlling the fuel cell heater, evaporation chambers on the anode and cathode sides.
- d) Back pressure valve
- e) Mass flow controller: MKS Type M100B
- f) Intake valve and relieve valve
- g) Pressure regulator

3.3 Analytical Instruments

1. Universal testing: LLOYD Instruments LR 5K (Department of Chemical Technology, Chulalongkorn University)
2. Potentiostat Galvanostat: AUTOLAB PGSTATO 30 (Department of Chemical Technology, Chulalongkorn University)
3. Compression molder: Labtech model LP20 (Department of Chemical Technology, Chulalongkorn University)
4. Scanning electron microscopy, JEOL model JSM-6400 (Scientific and Technological Research Equipment Center of Chulalongkorn University)
5. Energy Dispersive Spectroscopy, JEOL model JSM-6400 (Scientific and Technological Research Equipment Center of Chulalongkorn University)

3.4 Methodology

3.4.1 Membrane Preparation

- 1) Chitosan membrane
 - a) Dissolving 3 wt.% of chitosan flake in 3% acetic acid solution.
 - b) Stirring the mixture to be clear solution.
 - c) Leaving the solution at room temperature for eliminating the air bubbles.
 - d) Pouring 10 g. of solution and spreading uniformly on a 15×15 cm² glass plate.
 - e) Drying at 60°C for 6 hours.
 - f) Immersing the glass plate with membrane sheet in 4 wt.% of NaOH solution for 20 minutes.
 - g) Washing the membrane with water until neutral and drying at 60°C for 6 hours.
- 2) 10-30 wt.% Chitosan-zeolite composite membrane

- a) Adding 10-30 wt.% of zeolite in 3% acetic acid solution and stirring to be clear solution.
 - b) Dissolving 3 wt.% of chitosan flake in above solution and stirring to be clear solution.
 - c) Following the same procedure in 1) from steps c) to g).
- 3) Crosslinked chitosan membrane
- a) Immersing the chitosan membrane in 4 wt.% H_2SO_4 acid solution for 24 hours.
 - b) Washing the membrane with water and drying at room temperature.
- 4) Crosslinked chitosan-zeolite composite membrane
- a) Immersing the 10-30 wt.% Chitosan-zeolite composite membrane in 4 wt.% H_2SO_4 acid solution for 24 hours.
 - b) Washing the membrane with water and drying at room temperature.
- 5) Doped membrane
- a) Immersing the required membrane in 4 wt.% H_2SO_4 acid solution for 24 hours.
 - b) Absorbing the excess H_2SO_4 acid solution on membrane surface.

3.4.2 Tensile Strength Test

- 1) Cutting the membrane into a $5 \times 150 \text{ mm}^2$ strip.
- 2) Determining the membrane thickness with a micrometer.
- 3) Measuring the tensile strength following ASTM D882 with Universal testing machine (figure 3.2) at crosshead speed of 5 mm/min.

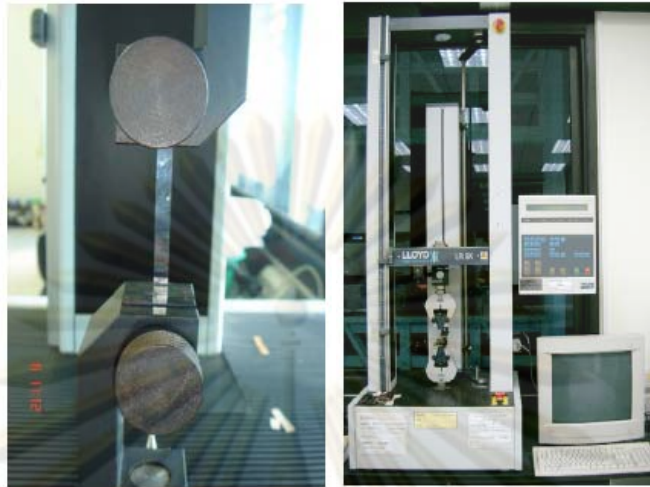


Figure 3.2 Universal testing LLOYD instruments LR 5K

3.4.3 Ion Exchange Capacity Test

- 1) Weighing the membrane approximately 20 mg.
- 2) Immersing the membrane in 25 ml (V_1) of 0.005 N (N_1) NaOH solution until equilibrium.
- 3) Pipetting the NaOH solution in 2) and titrating with 0.005 N (N_2) of HCl acid until pH 7.
- 4) Calculating the ion exchange capacity according to equation (3.1).

$$\text{Ion exchange capacity} = \frac{\left(N_1 V_1 - \left(\frac{V_1}{V_3} \right) N_2 V_2 \right)}{m} \quad (3.1)$$

N_1 = concentration of NaOH solution (Normal)

N_2 = concentration of HCl acid (Normal)

V_1 = volume of NaOH (ml)

V_2 = volume of HCl (ml)

V_3 = volume of NaOH used for titration (ml)

m = weight of membrane (g)

3.4.4 Constant Pressure Gas Permeability Test

- 1) Cutting the membrane into a circle with diameter 4 cm.
- 2) Assembling the membrane into the permeability cell as shown in Figure 3.3.
- 3) Controlling the permeability cell at 30, 60, or 90 °C.
- 4) Keeping the hydrogen gas pass through the permeability cell at 14.7 psi constantly.
- 5) Calculating the permeability in Barrer (1 Barrer = 10^{-10} (cm³ (STP)*cm)/(s*cm²*cmHg)) according to equation (3.2).

$$P = \frac{QL}{\Delta PA} \quad (3.2)$$

P = permeability coefficient (cm³ (STP)*cm)/(s*cm²*cmHg)

Q = flow rate of permeated hydrogen gas (scgs)

L = membrane thickness (cm)

ΔP = pressure difference (cmHg)

A = membrane surface area (cm²)



Figure 3.3 Gas permeability test unit

3.4.5 Membrane Proton Conductivity by Four Probe Method

- 1) Cutting the membrane into a $1 \times 4 \text{ cm}^2$ strip and immersing in distilled water for 10 min. for preconditioning.
- 2) Placing the membrane on the platinum wires as shown in figure 3.4.
- 3) Placing two $1 \times 2.5 \text{ cm}^2$ platinum plates on both ends of the membranes.
- 4) Placing the assembled cell into the control chamber.
- 5) Flowing the 100% humid hydrogen gas or nitrogen gas into the control chamber.
- 6) Controlling the temperature control chamber at 30, 60, or 90°C .
- 7) Supplying the direct current through a platinum plate and measuring the voltage between two platinum wires.
- 8) Converting into the resistivity and calculating the proton conductivity according to equation 3.3.

$$\sigma = \frac{1}{R} \left(\frac{L}{A} \right) \quad (3.3)$$

σ = proton conductivity (Siemens/cm)

R = resistivity (Ohm)

L = distance between the platinum electrodes (cm)

A = cross section area of membrane (cm^2)

ศูนย์วิทยทรัพยากร

จุฬาลงกรณ์มหาวิทยาลัย

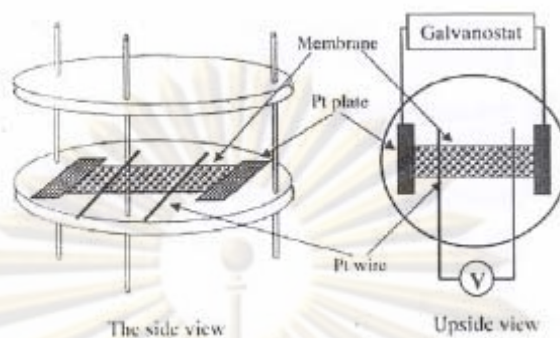


Figure 3.4 Schematic diagram of proton conductivity measurement by four probes technique

3.4.6 Coating of Catalyst Layer on the Membrane by Electroless Plating Technique

- 1) Preparing the platinum catalyst solution with recipe as shown in table 3.1.

Table 3.1 Catalyst solution for electroless plating

PtCl ₂	5 g/L
Na ₂ EDTA	40.1 g/L
NH ₃ ·H ₂ O (28 %w/w)	198 ml/L
N ₂ H ₄ (99.5 %w/w)	6 ml/L
Total volume	1 L

- a) Dissolving 5 g. of Pt(II)Cl₂ in 1 L of Na₂EDTA in ammonia solution and keeping as stock solution.
 - b) Adding hydrazine in the stock solution whenever ready for coating.
- 2) Coating procedure
 - a) Dropping the catalyst solution into the 7X7 cm² teflon mold having the reservoir area same as MEA size (2.3X2.3 cm²) as shown in figure 3.5.

- b) Placing a $7 \times 7 \text{ cm}^2$ membrane sheet on the teflon mold and covering with a glass plate.
- c) Controlling the teflon mold at 60°C for 90 min as previously reported [5].
- d) Following the same procedure on the other side of membrane.
- e) Washing the membrane with distilled water and drying at room temperature



Figure 3.5 Teflon mold for electroless plating

3.4.7 Characterizations of Plated Membrane

- 1) Dispersion of platinum particle on the membrane surface by Scanning Electron Microscopy (SEM).
- 2) Analyzing the platinum amount on membrane by Energy Dispersive Spectroscopy (EDS).
- 3) Membrane proton conductivity by four probes method.

3.4.8 Preparation of Membrane/Electrode Assembly (MEA)

- 1) Applying 3 wt% chitosan solution on two carbon papers sizing $2.3 \times 2.3 \text{ cm}^2$ used as electrodes of MEA.
- 2) Coupling the carbon papers on both sides of the plated membrane.

- 3) Covering the outer part of the MEA with high thermally stable polymer sheets and metal plates.
- 4) Pressing by a Compression Molder at a pressure of 30 kg/cm^2 and in the temperature range of $30\text{-}47 \text{ }^\circ\text{C}$ for 1 min as previously reported [5].

3.4.9 Proton Conductivity in a Single Cell

- 1) Assembling the MEA into a single fuel cell unit as shown in figure 3.6.
- 2) Placing the single cell in the control chamber.
- 3) Flowing the 100% humid hydrogen gas into the anode side of the fuel cell.
- 4) Flowing the air into the cathode side of the fuel cell.
- 5) Controlling the temperature of chamber at 30, 60, or 90°C .
- 6) Measuring the MEA resistivity in the fuel cell and calculating the proton conductivity according to equation 3.3.



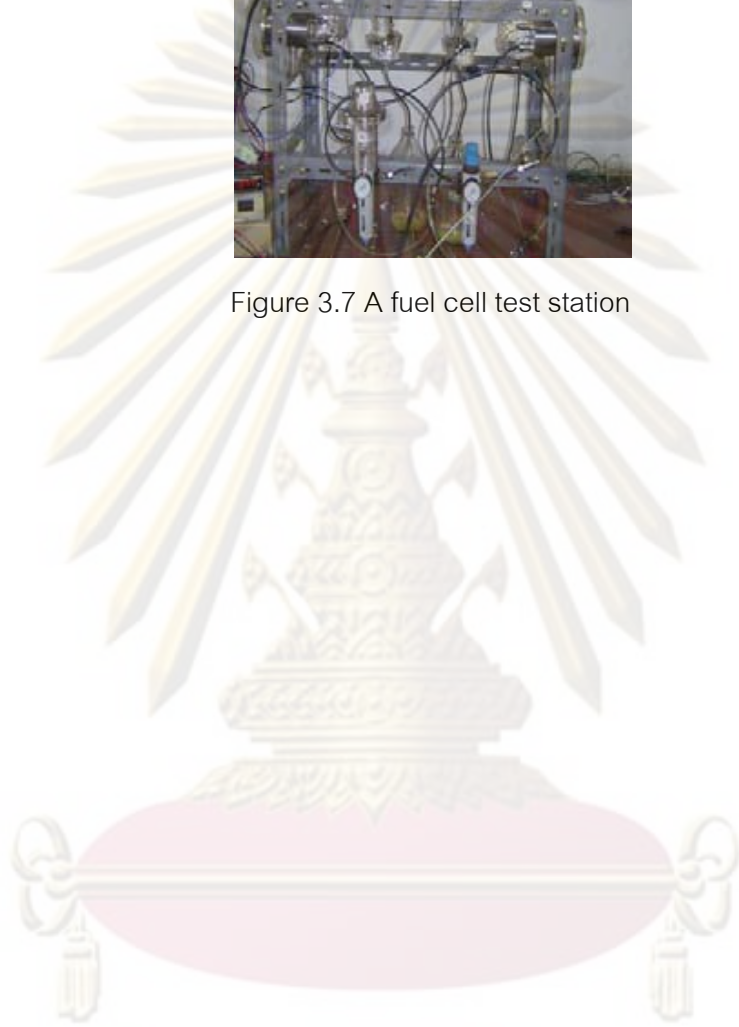
Figure 3.6 Single fuel cell unit

3.4.10 Performance Testing of a Single Fuel Cell

- 1) Assembling the MEA into the single cell unit.
- 2) Installing the fuel cell unit to the test station of figure 3.7 and connecting the gas inlet and outlet lines.
- 3) Following the procedures as stated in the manual.
- 4) Measuring the polarization using GPES program.



Figure 3.7 A fuel cell test station



ศูนย์วิจัยทรัพยากร
จุฬาลงกรณ์มหาวิทยาลัย

CHAPTER IV

RESULTS AND DISCUSSION

4.1 Basic properties of materials and membranes

The properties of chitosan and zeolite used in this research are shown in table 4.1. The molecular weight and %deacetylation of chitosan were 9.5×10^5 dalton and 90.0 ± 5.0 , respectively. The Si:Al ratio of 1.1 was of zeolite A. The pore size, surface area, and pore volume were 6.7 Å, 522.98 m²/g, and 0.3069 cm³/g, respectively.

Table 4.1 Properties of chitosan and zeolite A

Property	Chitosan (*)	Zeolite A (**)
Molecular weight (Dalton)	9.5×10^5	--
Weight % Deacetylation	90.0 ± 5.0	--
Counter ion	--	Na ⁺
SiO ₂ /Al ₂ O ₃	--	1.1
Pore size (Å)	--	6.7
Surface area (m ² /g)	--	522.98
Pore volume (cm ³ /g)	--	0.3069

* Information from ELAND LTD.

** From previous study [2]

Table 4.2 Thickness of membranes

Type of membranes	Thickness (mm)
Nafion	0.199±0.005
Uncrosslinked membranes	0.061±0.007
Crosslinked membranes	0.072±0.007
Doped membranes	0.053±0.006

4.2 Tensile strength

The tensile strength of crosslinked chitosan-zeolite composite and sulfuric acid doped crosslinked composite membrane are shown in Figure 4.1. It was found out that the tensile strength of crosslinked chitosan-zeolite composite membranes decreased from 62.5±0.86 to 40.2±0.75 MPa when zeolite content increased from 0% to 30%. This showed that zeolite particles were dispersed in the chitosan chains. (Too high of zeolite content, the tensile strength was depreciated rapidly). However, all crosslinked chitosan-zeolite composite membranes were better than Nafion[®]117 membrane (28.4±2.3 MPa).

The sulfuric acid solution absorbed in the doped membranes worsened the tensile strength of the membranes. Only 0% zeolite doped crosslinked membrane (29.6±1.15 MPa) was comparable to Nafion[®]117 membrane.

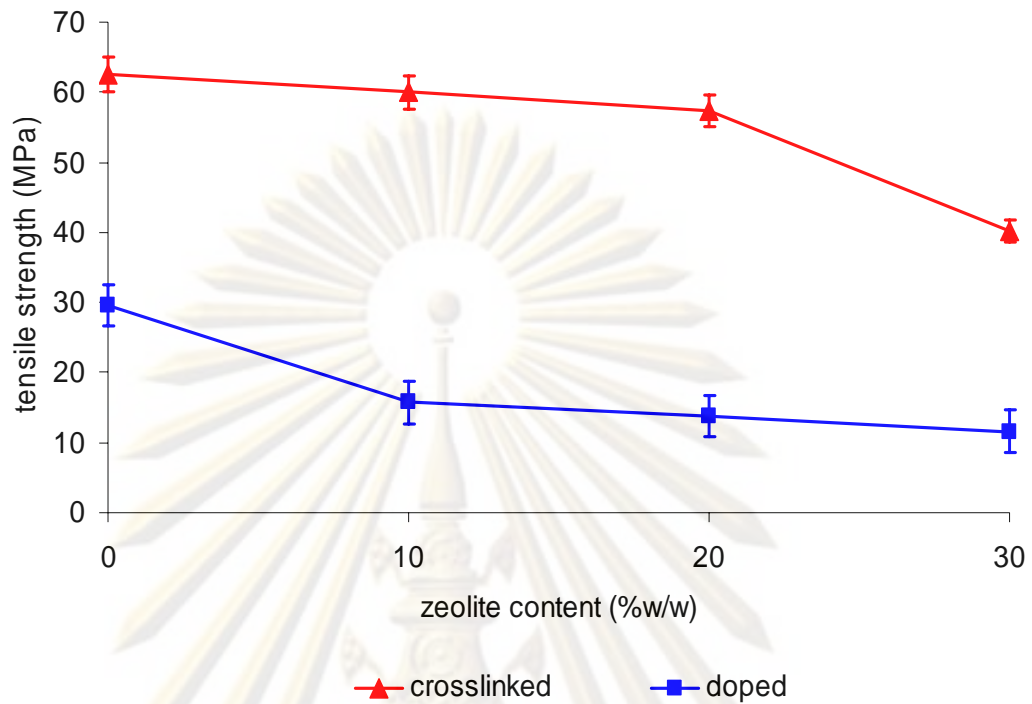


Figure 4.1 Tensile strength of crosslinked chitosan-zeolite membrane and sulfuric acid doped crosslinked membrane

4.3 Ion exchange capacity

The net charges in zeolite A were negative due to the tetrahedron bonds of Si, Al and 4 atoms of oxygen. Furthermore, the functional groups in crosslinked chitosan membrane were consisted of -OH^- , -NH_3^+ and -SO_4^{2-} groups. The ion exchange capacity was thus increased from 3.43 ± 0.05 meq/g to 3.71 ± 0.05 meq/g as shown in Figure 4.2 when the amount of zeolite in crosslinked chitosan-zeolite membranes were increased from 0 to 30% by weight. Whereas the Nafion[®]117 membrane contained only $\text{-SO}_3\text{H}$ group showed the ion exchange capacity of 1.01 ± 0.11 meq/g. The high ion exchange capacity of crosslinked chitosan membranes showed the potentiality as the proton exchange membranes. Nevertheless, the ion exchange capacity was only a preliminary indicator; the better parameter, proton conductivity, should be investigated.

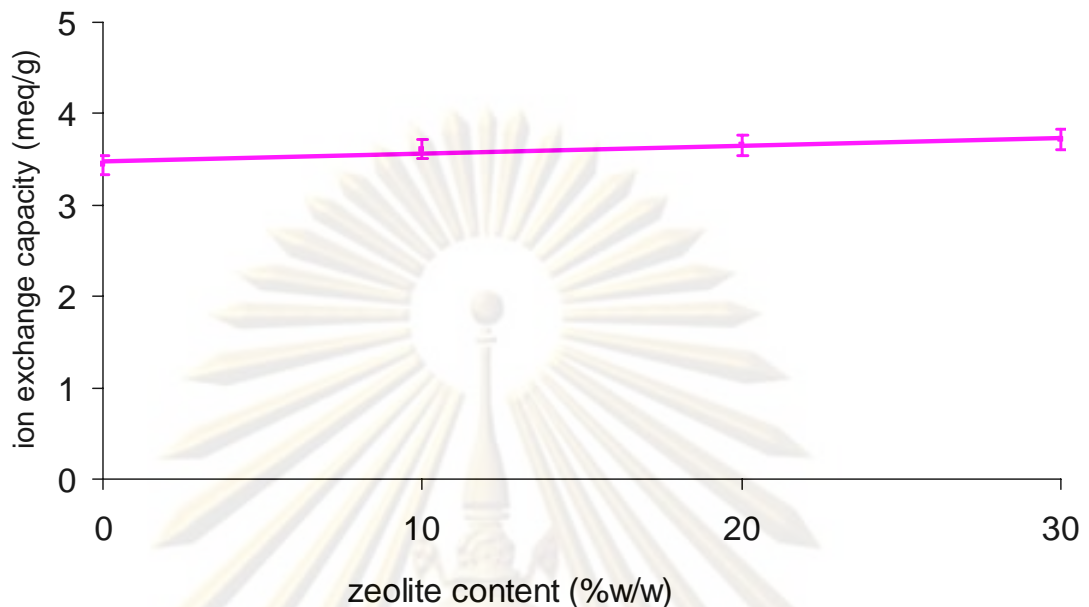


Figure 4.2 Ion exchange capacity of crosslinked chitosan membrane

4.4 Gas permeability

The high permeability of H_2 and O_2 could cause explosion in the fuel cell on the fire triangle principle. According to the Knudsen diffusion, it was believed that the smaller the gas molecule, the more permeability of the gas was. Only the H_2 permeability was studied in this research. Figure 4.3 showed the H_2 permeability at 30, 60 and 90°C of uncrosslinked and crosslinked chitosan-zeolite composite membranes comparing to that of Nafion[®]117 membrane. It was found that the H_2 could permeate through the chitosan based membranes much less than Nafion[®]117 membrane. The addition of zeolites in the membrane caused the gas transportation path longer and more complexity; additionally the flexibility and free volume of the polymer chains were reduced. The H_2 permeability was lessened with the increase in zeolite contents. The stiffer [41] and denser [42] of crosslinked chitosan membranes than the uncrosslinked membranes lessened the permeability. The higher H_2 permeability due to temperature effect could be explained that the increased temperature caused higher kinetic energy of the gas molecules and larger free volume of the polymer chains.

The H₂ permeability of 30% crosslinked chitosan-zeolite composite membrane at 30, 60 and 90°C was 650±0.65, 790±0.64 and 987±0.60 Barreres, respectively. That of Nafion[®] 117 membrane at respective temperature was 6100±67, 6902±84, and 7305±128 Barreres, respectively.

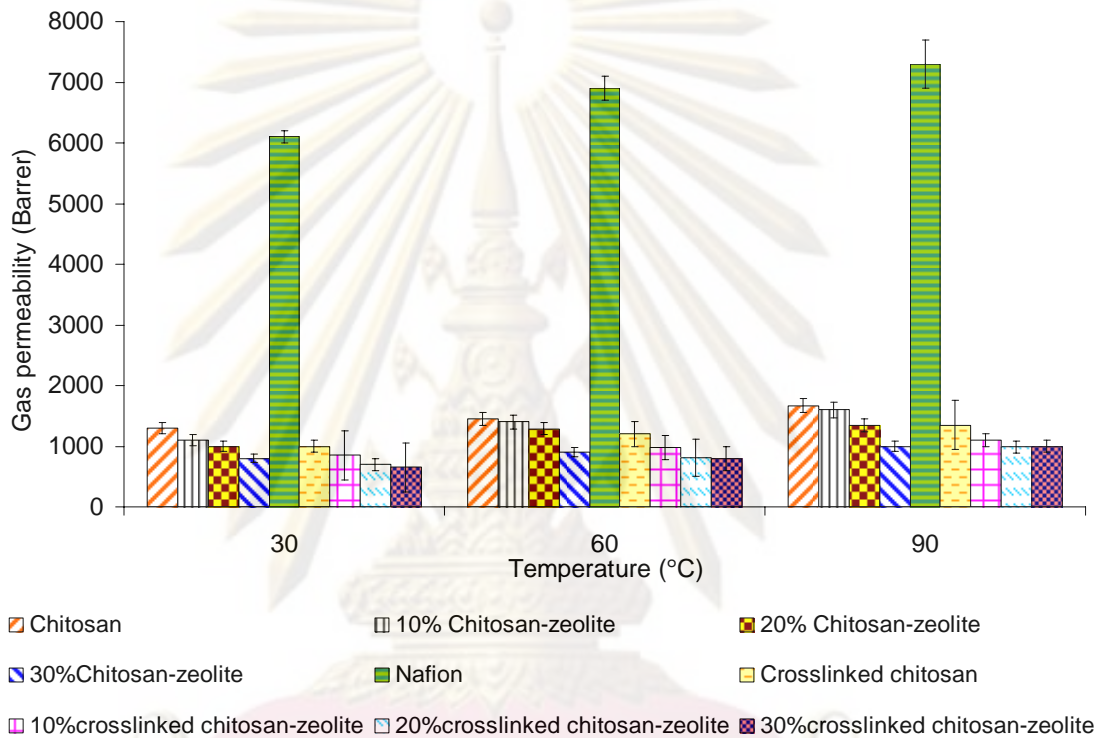


Figure 4.3 H₂ permeability of crosslinked and uncrosslinked chitosan-zeolite composite membranes at various temperatures

The effect of sulfuric acid doping on H₂ permeability of crosslinked chitosan-zeolite membrane is shown in Figure 4.4. It showed that the increase in H₂ permeability was obtained. This indicated that wetting the chitosan based membranes either by water or sulfuric acid solution could expand the free volume of polymer chains. However, the H₂ permeability of all doped membranes was still lower than that of commercial Nafion[®] 117 membrane at all range of temperatures. The H₂ permeability of 30% doped

crosslinked chitosan-zeolite composite membrane at 30, 60 and 90°C was 1033 ± 0.35 , 1230 ± 0.32 and 1340 ± 0.34 Barreres, respectively.

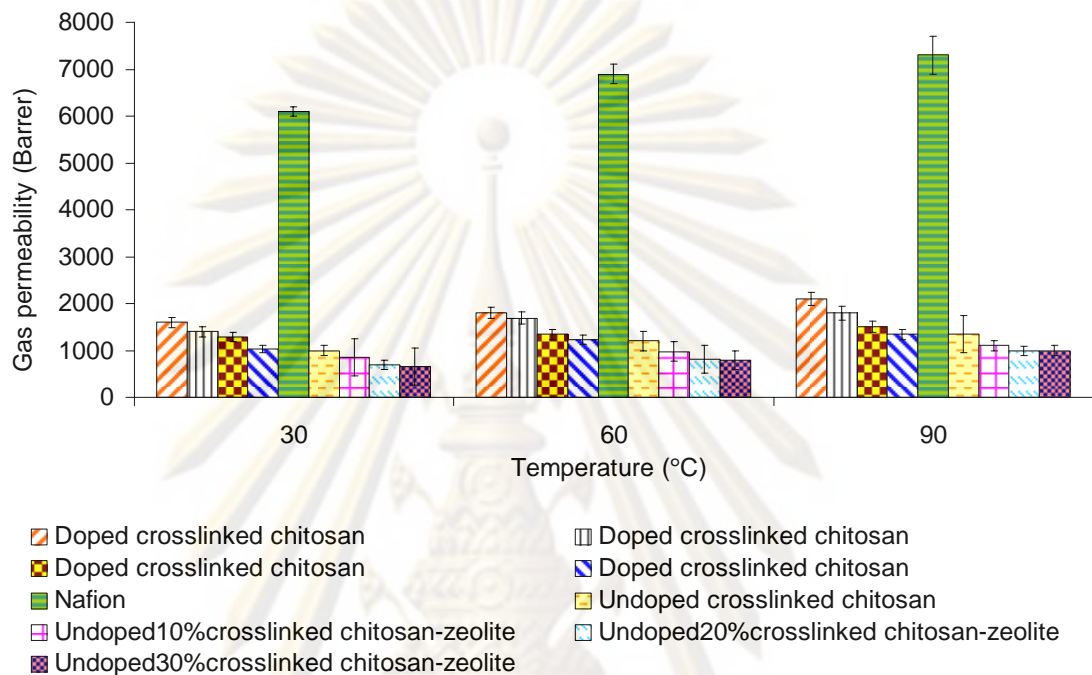


Figure 4.4 Effect of sulfuric acid doping on H_2 permeability of crosslinked chitosan-zeolite membrane at various temperature

Since the hydrogen feed gas in normal proton exchange membrane fuel cell must be hydrated as hydronium (H_3O^+) transportation; the H_2 permeability in the 30% crosslinked chitosan-zeolite composite membrane at various gas and membrane conditions was studied with the results shown in Figure 4.5. It showed that the water molecules carried by the hydrated gas were sufficient for expanding the free volume of polymer chains due to high hydrophilicity of the membrane causing the increased H_2 permeability. However, using initially the water hydrated membrane could enhance the H_2 permeability much more than the former. This was due to the water swelling effect of crosslinked chitosan-zeolite composite membrane whilst the gas molecule size was not changed much. It was found out that the H_2 permeability of 30% doped crosslinked

chitosan-zeolite composite membrane (1033 ± 1.22 Barreres, respectively) was closed to the condition using hydrated gas but dry membrane (980 ± 1.29 Barreres, respectively) than the condition using hydrated gas and hydrated membrane at all range of temperatures (1450 ± 1.32 Barreres, respectively). This could be stated that the chitosan membranes possessed very high hydrophilicity. It might take an advantage of this property on self humidification operation without external humidifier and/or high temperature operation of fuel cell.

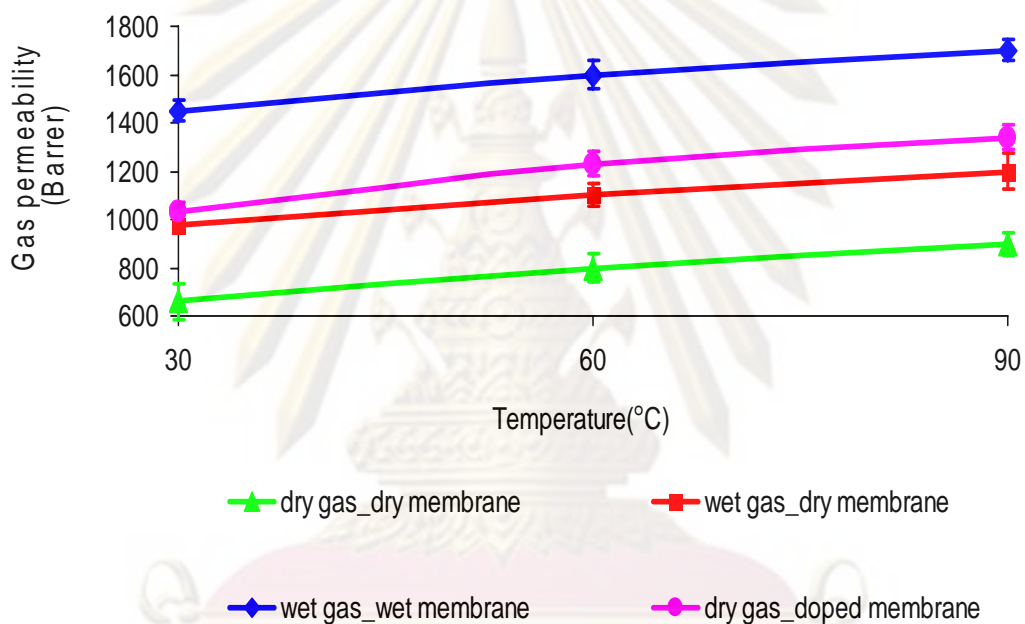


Figure 4.5 H₂ permeability of 30% crosslinked chitosan-zeolite composite membrane at various conditions

4.5 Membrane Proton Conductivity

Figure 4.6 shows the membrane proton conductivity of uncrosslinked and crosslinked chitosan-zeolite membrane at room temperature (30°C). As expected, the proton conductivity of crosslinked membranes was higher than that of uncrosslinked membranes. This could be explained that the SO₄²⁻ groups in crosslinked membranes facilitated the proton transport same as the phenomena at SO₃²⁻ groups in Nafion membrane. It was observed that the proton conductivity of both uncrosslinked and

crosslinked chitosan-zeolite membrane increased with zeolite contents. The increased net negative charges of zeolites might play this role.

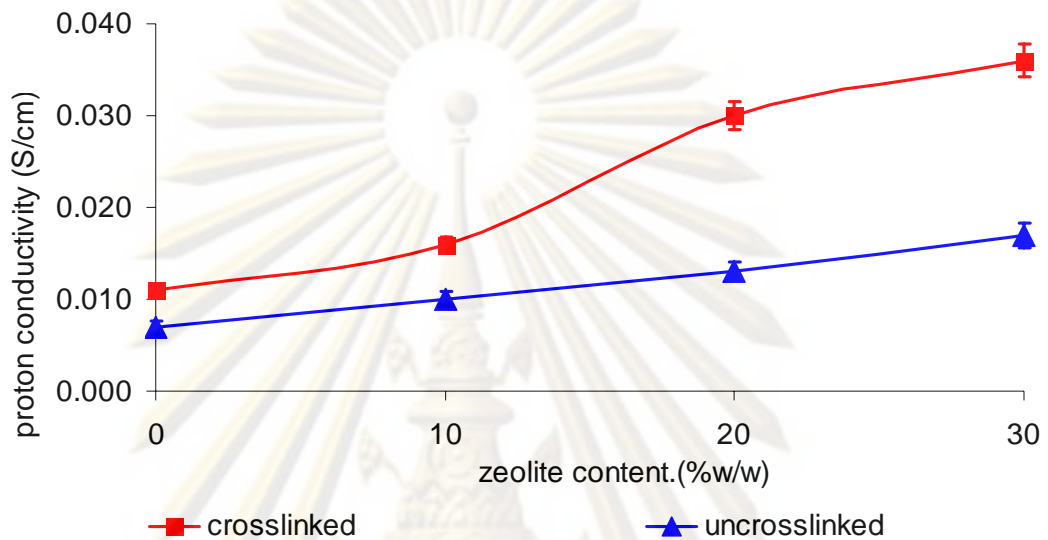


Figure 4.6 Proton conductivity of uncrosslinked and crosslinked chitosan-zeolite composite membrane at room temperature (30°C)

The effect of temperature on proton conductivity is shown in Figure 4.7. The proton conductivity of either crosslinked chitosan-zeolite composite membranes or Nafion[®]117 membrane increased correspondingly with temperature according to kinetic energy principle. The proton conductivity of Nafion[®]117 membrane at 30, 60, and 90°C as shown in table 4.3 was 0.057 ± 0.005 , 0.069 ± 0.004 and 0.072 ± 0.002 S/cm, respectively. Same as previous studies [5], the sulfuric acid solution absorbed in the doped crosslinked chitosan-zeolite composite membranes could enhance the proton conductivity over that of Nafion[®]117 membrane as shown in Figure 4.8. This was due to the strong electrolyte action of sulfuric acid solution. The proton conductivity of doped crosslinked chitosan-zeolite composite membranes at 30°C was increased from 0.070 ± 0.011 S/cm to 0.105 ± 0.010 S/cm when the zeolite content was increased from 0% to 30%.

It should be noted that the membrane proton conductivity measured by four probes method in this section was on the membrane surface plane. Although the proton transport in the fuel cell was perpendicular to the membrane surface passing through the membrane thickness, the measurement of membrane proton conductivity by four probes method was still acceptable for the scientists in the art.

Table 4.3 Proton conductivity of Nafion[®] 117 membrane

Temperature (°C)	Proton conductivity (S/cm)
30	0.057±0.005
60	0.069±0.004
90	0.072±0.002

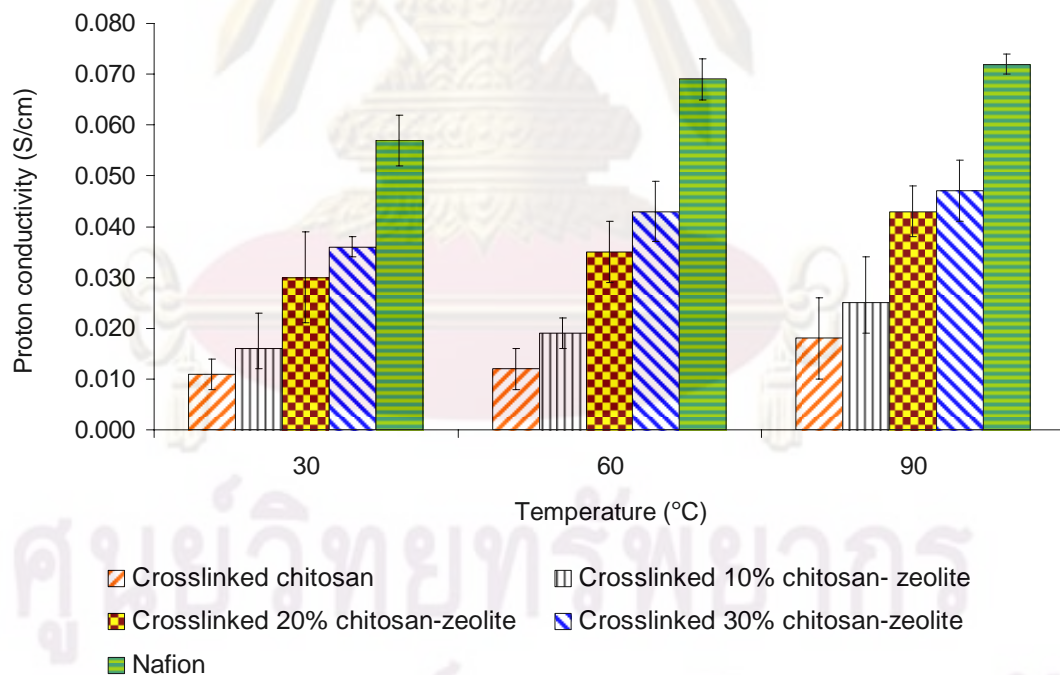


Figure 4.7 Proton conductivity of crosslinked chitosan-zeolite membrane and Nafion membrane at various temperatures

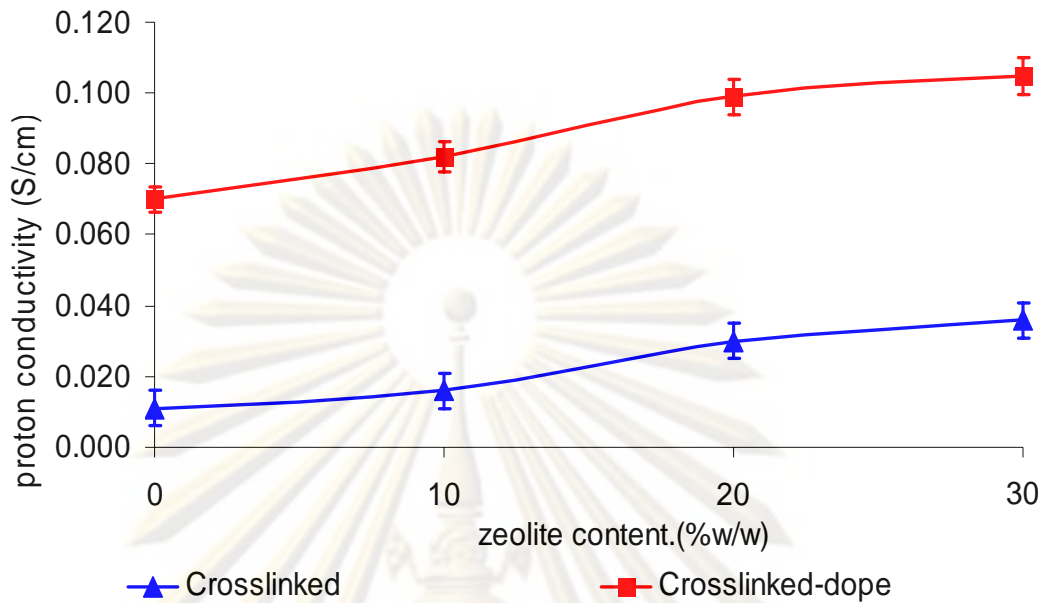


Figure 4.8 Proton conductivity at 30°C of doped and undoped crosslinked chitosan-zeolite membrane

To prove that the obtained values were of proton conductivity indeed, N₂ instead of H₂ gas was fed. The conductivity of crosslinked chitosan-zeolite and Nafion[®]117 membranes fed by H₂ or N₂ gas at 30, 60, and 90°C is shown comparatively in Figure 4.9. It showed clearly that the conductivity at each temperature of all membranes in N₂ atmosphere was much lower than that of in H₂ atmosphere. The obtained conductivity measured in N₂ atmosphere might be the electron conductivity. It could be explained from two hypotheses; i.e., the platinum could dissociate specifically only the H₂ molecule into proton (H⁺) and electron and the successive result from supplied currents in measurement procedure. The conductivity difference from both atmospheres should be the real membrane proton conductivity. However, the error was small enough to report values obtained from H₂ atmosphere.

The conductivity of 30% crosslinked chitosan-zeolite membrane in N₂ atmosphere at 30, 60 and 90°C was 0.005±0.002, 0.006±0.006 and 0.008±0.006 S/cm, respectively. That of Nafion[®]117 membrane was 0.006±0.0050, 0.008±0.004 and

0.009±0.002 S/cm, respectively. It could be stated that the crosslinked chitosan-zeolite membranes were electron conductive less than Nafion[®]117 membrane.

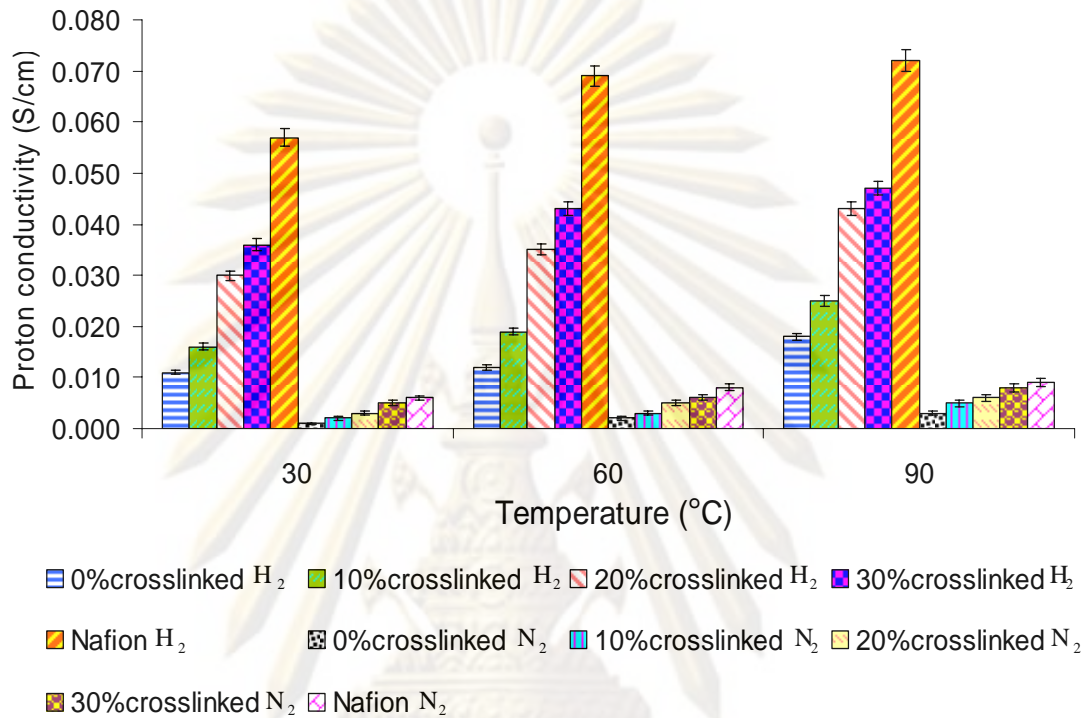
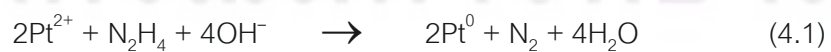


Figure 4.9 Comparison of membrane conductivity measured by four probes method feeding with nitrogen gas and hydrogen gas of various membranes and temperatures

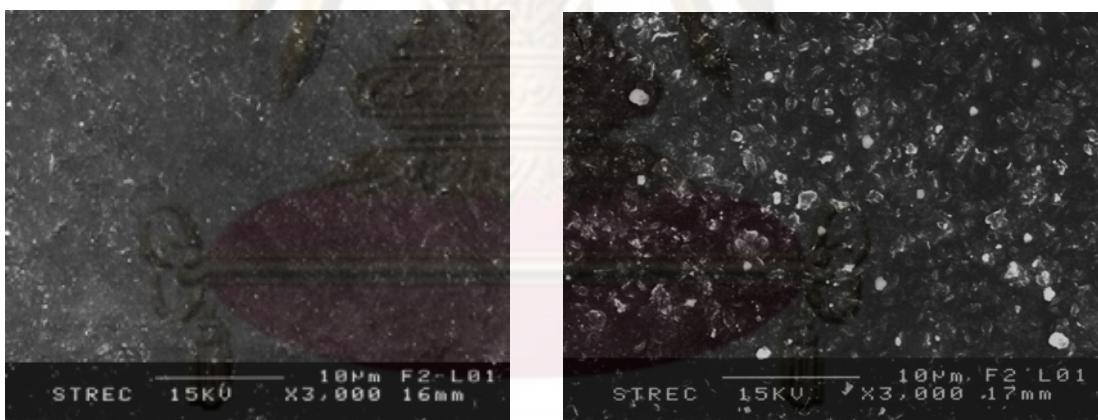
4.6 Platinum Plated Chitosan Based Membranes

The platinum was necessarily used as a catalyst for proton exchange membrane fuel cell especially at the anode side. The electroless plating was based on an autocatalytic reaction as shown in equation 4.1 through the reduction-oxidation reaction of Pt ion and hydrazine on the catalytic surface of the membrane.



4.6.1 Morphology and Platinum Loading

The surface morphology of 30% crosslinked chitosan-zeolite composite membrane before and after plating at 60°C for 90 minutes is shown in Figure 4.10. It was observed that there were some particles attached on the membrane surface. From the EDX spectrum in Figure 4.11, it could be confirmed that the particles found on the membrane surface were platinum. The approximate calculation of platinum loading in various chitosan based membranes in this study is shown in table 4.4. The lower platinum loading of uncrosslinked chitosan based membranes indicated that the catalytic sites of uncrosslinked chitosan based membranes should be only at nitrogen atom in amine groups due to its electron lone pairs. On the other hand, the catalytic sites in crosslinked chitosan based membranes should be ones having negative charge; e.g., -OH^- , -SO_4^{2-} groups and tetrahedron bonds of Si, Al and oxygen of zeolite.



(a)

(b)

Figure 4.10 Surface morphology of 30% crosslinked chitosan-zeolite composite membrane at a magnification of 3,000 (a) before plating (b) after plating

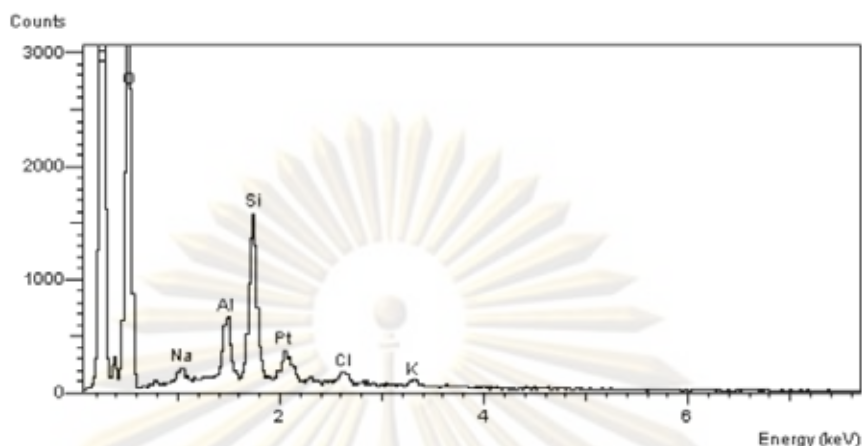


Figure 4.11 EDX spectrum of 30% crosslinked chitosan-zeolite composite membrane after electroless plating at 60°C for 90 minutes

Table 4.4 Platinum loading on the membrane surface

Type of membrane	Zeolite content (wt%)	%Pt
Crosslinked chitosan zeolite composite membrane	0	0.70
	10	1.02
	20	1.11
	30	1.80
Uncrosslinked chitosan zeolite composite membrane	0	0.15
	10	0.28
	20	0.46
	30	0.52

4.6.2 Proton Conductivity of Platinum-plated Membrane

It was found that after plating the proton conductivity in all membranes was increased even much higher than that of Nafion[®]117 membrane at all range of temperatures as shown in Figure 4.12. As seen in Figure 4.13 that the proton conductivity in sequence at all ranges of temperatures were as follows: plated doped

chitosan > plated crosslinked chitosan > plated uncrosslinked chitosan > Nafion[®] 117 > nonplated crosslinked chitosan. This confirmed that the platinum plating on membranes was successful.

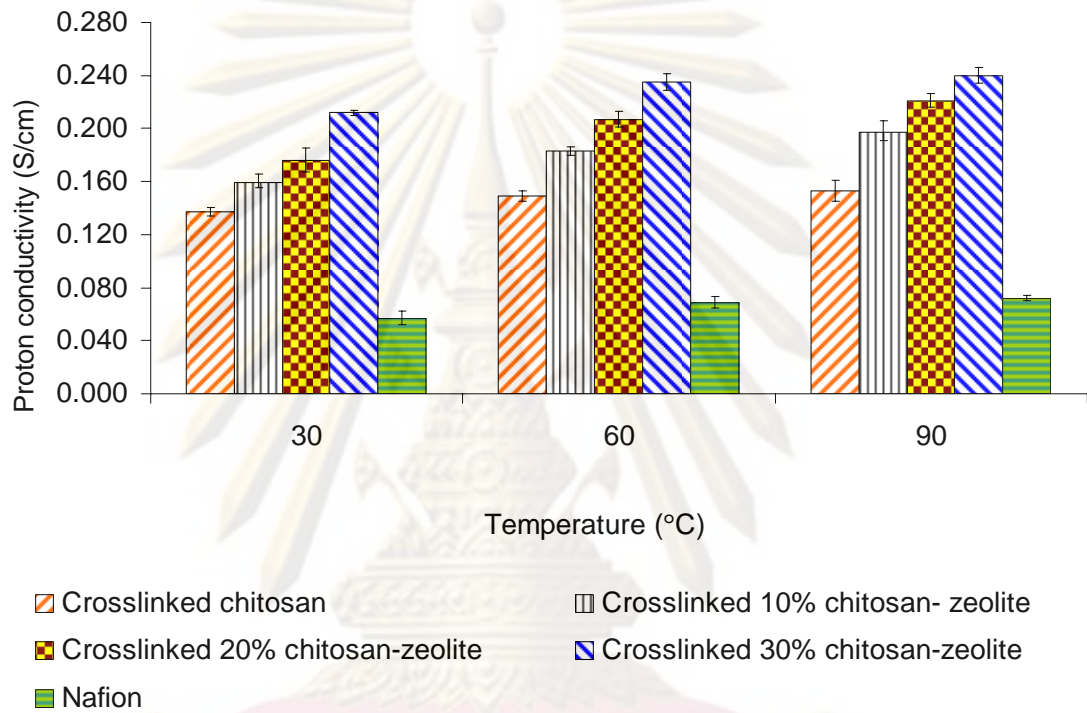


Figure 4.12 Membrane proton conductivity of platinum-plated crosslinked chitosan-zeolite membrane at various temperatures

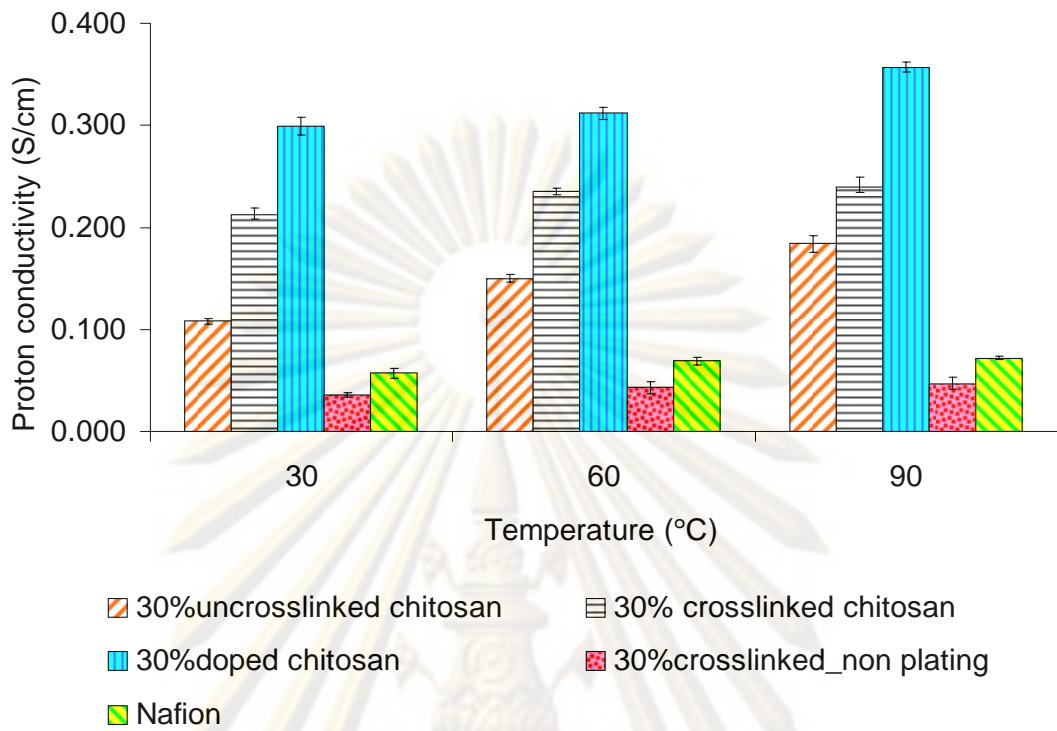


Figure 4.13 Comparison of membrane proton conductivity at 30% zeolite contents in various membrane types and temperatures after plating at 60°C for 90 minutes

ศูนย์วิทยทรัพยากร
จุฬาลงกรณ์มหาวิทยาลัย

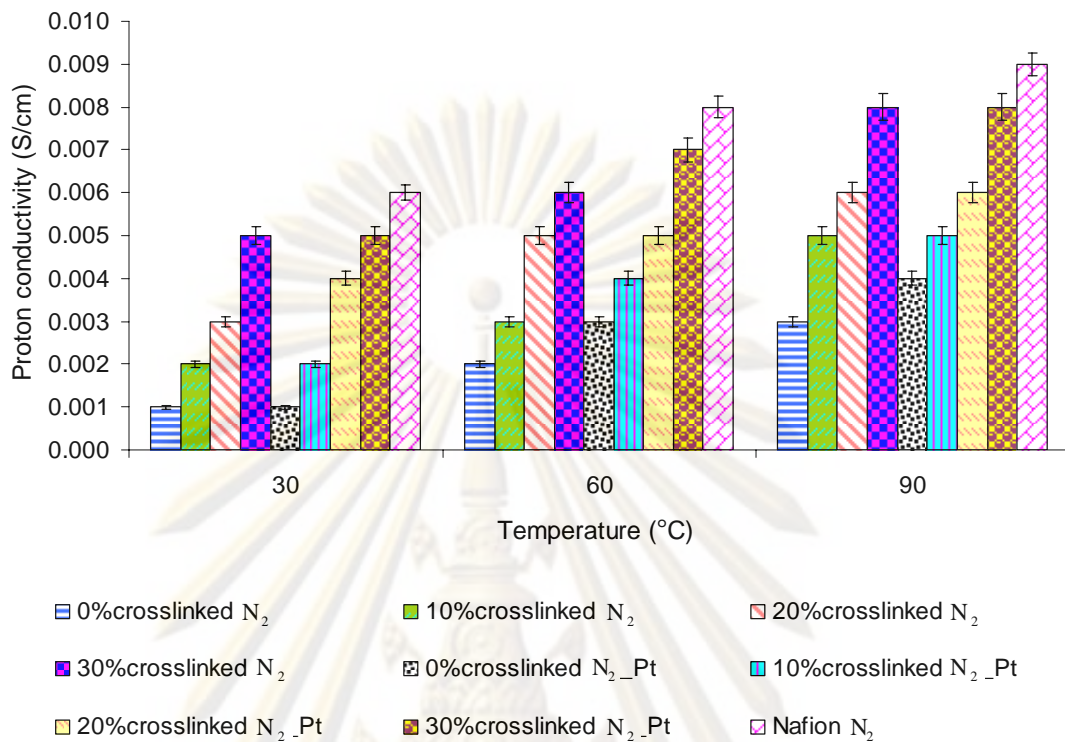


Figure 4.14 Electron conductivity of unplated and plated membranes in nitrogen atmosphere at various temperatures

The electron conductivity measured in nitrogen atmosphere of plated crosslinked chitosan composite membranes compared with that of unplated crosslinked chitosan composite membranes and Nafion[®]117 membrane is shown in Figure 4.14. It could be stated that i) the electron conductivity of Nafion[®]117 membrane showed highest at all ranges of temperatures, ii) the higher the zeolite contents, the higher the electron conductivity, iii) the electron conductivity was increased with temperature, iv) the electron conductivity of plated crosslinked chitosan composite membranes was comparable to that of unplated membranes at 30°C but the difference was bigger with increased temperature, and v) the electron conductivity of plated membranes showed generally higher than of unplated membranes. The high electron conductivity or high electron transport might cause a short circuit in the fuel cell that should be avoided. It was thus a required membrane property for the proton exchange membrane fuel cell.

4.6.3 H₂ Permeability

The effect of Pt plating on the H₂ permeability is shown in Figure 4.15. The H₂ permeability of plated 30% crosslinked chitosan-zeolite membrane was slightly lower than that of unplated membrane. This could be due to the gas path blocking of platinum particles. Nevertheless, the Pt loading was not so high that the H₂ permeability could be affected significantly. The same trend was obtained in all testing conditions except the lower gas permeability.

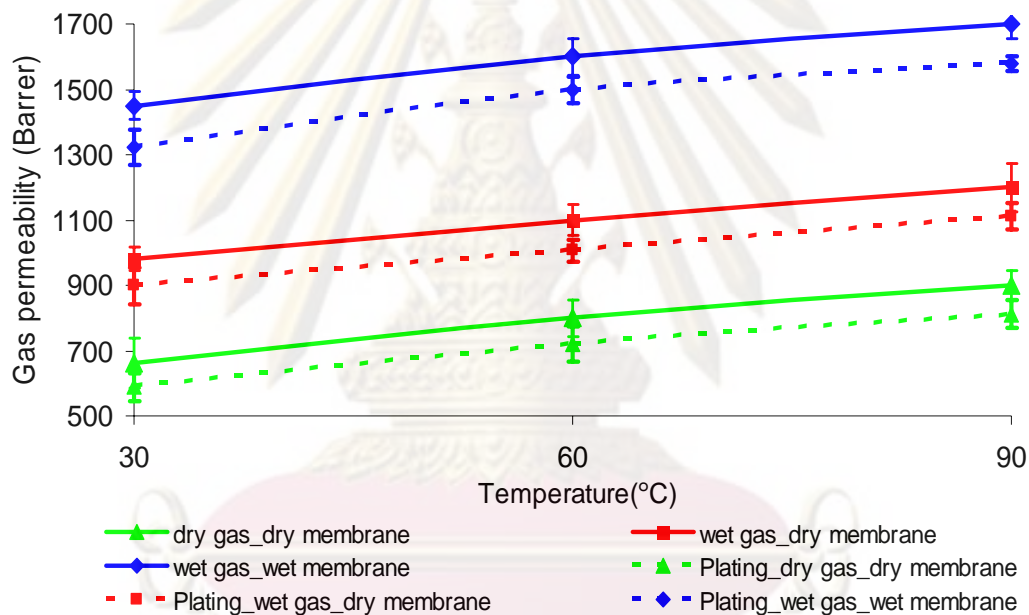


Figure 4.15 Comparison in H₂ permeability at various conditions and temperatures of plated and unplated 30% crosslinked chitosan-zeolite membrane

4.7 Proton Conductivity in a Single Cell

As stated earlier in Section 4.5 above, the proton transport in the fuel cell was perpendicular to the membrane surface through the membrane thickness. The membrane electrode assembly (MEA) of 30% uncrosslinked chitosan-zeolite, 30% crosslinked chitosan-zeolite, and 30% doped crosslinked chitosan-zeolite membranes

was assembled in a single cell and tested by four probes technique for proton conductivity as shown in Figure 4.16. Whilst the proton conductivity of commercial MEA from Electrochem Inc. (having Pt loading of 0.5 mg/cm^2) at 60°C was $0.048 \pm 0.006 \text{ S/cm}$, those of MEA from above three chitosan based membranes at the same temperature were 0.013 ± 0.002 , 0.016 ± 0.002 , and $0.040 \pm 0.010 \text{ S/cm}$, respectively. It was found that only the MEA prepared from 30% doped crosslinked chitosan-zeolite membrane was comparable to the commercial MEA. The proton conductivity of MEA prepared from various zeolite contents of doped crosslinked chitosan-zeolite membrane is shown in Figure 4.17 comparing with the values obtained from the planar view. It showed clearly that the proton conductivity in cross section view was much lower than that in the planar view. It was interesting that the proton conductivity of Nafion[®] 117 membrane in the planar view was not much higher than that of commercial MEA in the cross sectional view. This might be due to the exact plating loading as well as the good compactness of the commercial MEA. The lower proton conductivity of MEA in the cross sectional view was due to the increased resistance of connection between graphite plate and membrane and of graphite plate itself. The proton conductivity was only a screening parameter; the polarization curve was more acceptable for determining fuel cell performance.

ศูนย์วิทยทรัพยากร
จุฬาลงกรณ์มหาวิทยาลัย

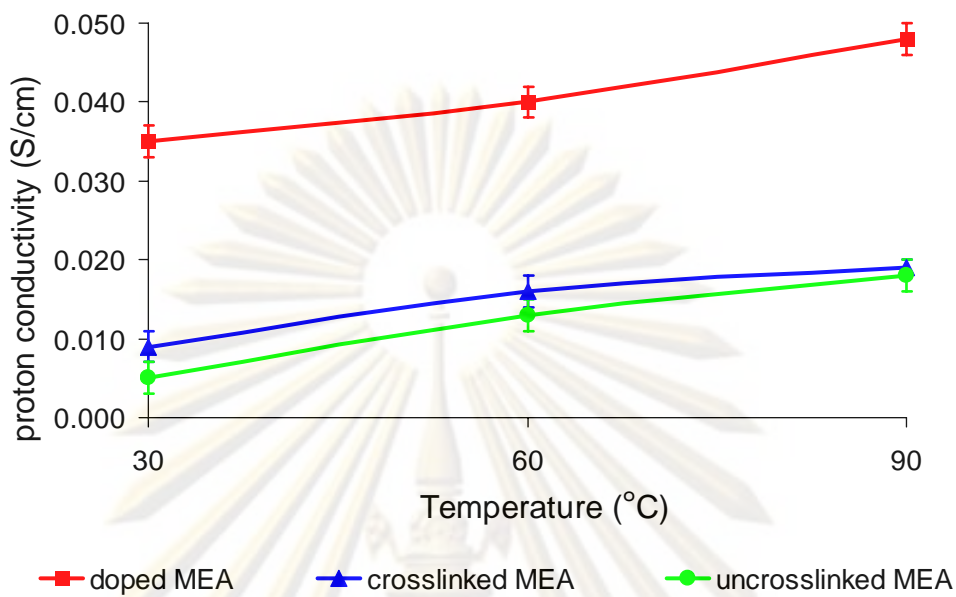


Figure 4.16 Cross sectional proton conductivity of 30% zeolite contents MEA in fuel cell at various membrane types and temperatures

ศูนย์วิทยทรัพยากร
จุฬาลงกรณ์มหาวิทยาลัย

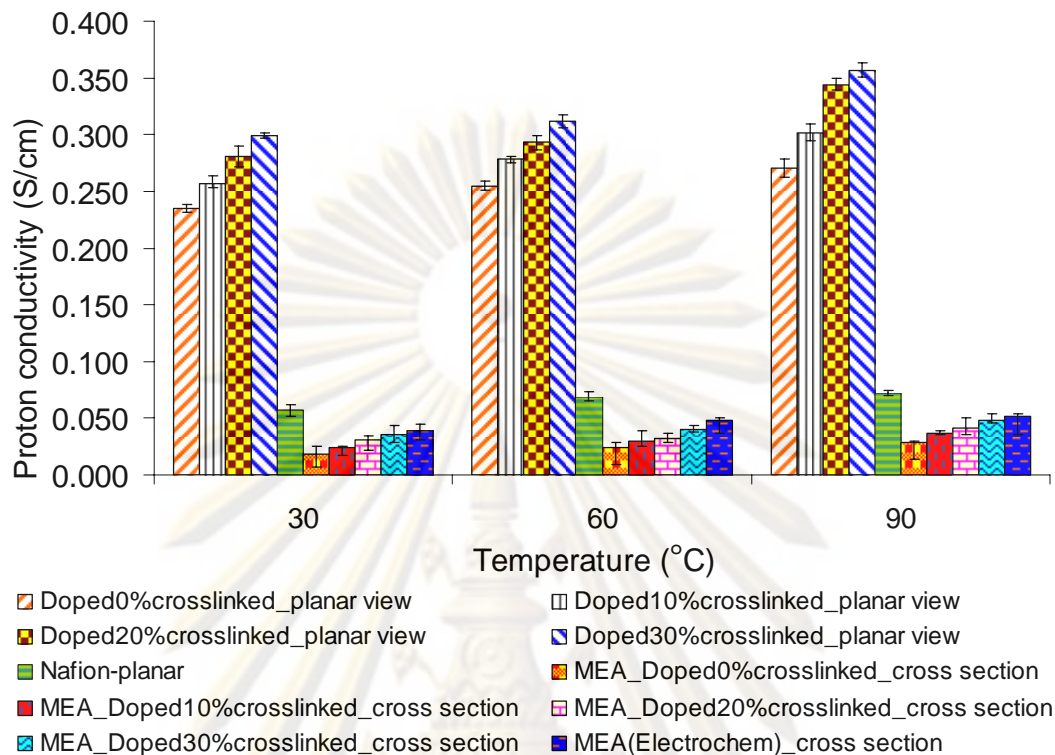


Figure 4.17 Comparison of proton conductivity in planar view and of MEA in fuel cell of doped crosslinked chitosan-zeolite membrane at various temperatures

4.8 Effect of Relative Humidity on the Fuel Cell Performance

The polarization at 30°C and various relative humidity of MEA prepared from 30% zeolite contents of uncrosslinked, crosslinked and doped crosslinked chitosan-zeolite membrane is shown in Figure 4.18, 4.19 and 4.20, respectively. It was found that the best performance was obtained from those three chitosan based MEA at zero hydrated feed gas in both anode and cathode sides (RH 0%-0%) whilst the worst performance was obtained at fully hydration in both sides (RH 100%-100%). The polarization at zero hydration in both anode and cathode sides (RH 0%-0%) of those three MEA was replotted in Figure 4.21. It showed that the MEA from 30% doped crosslinked chitosan-zeolite membrane was the best corresponding to the proton conductivity results. The current density at 0.5 V of those three MEA was 1.9 ± 0.1 , 5.1 ± 0.1 , and 9.5 ± 0.01 mA/cm², respectively.

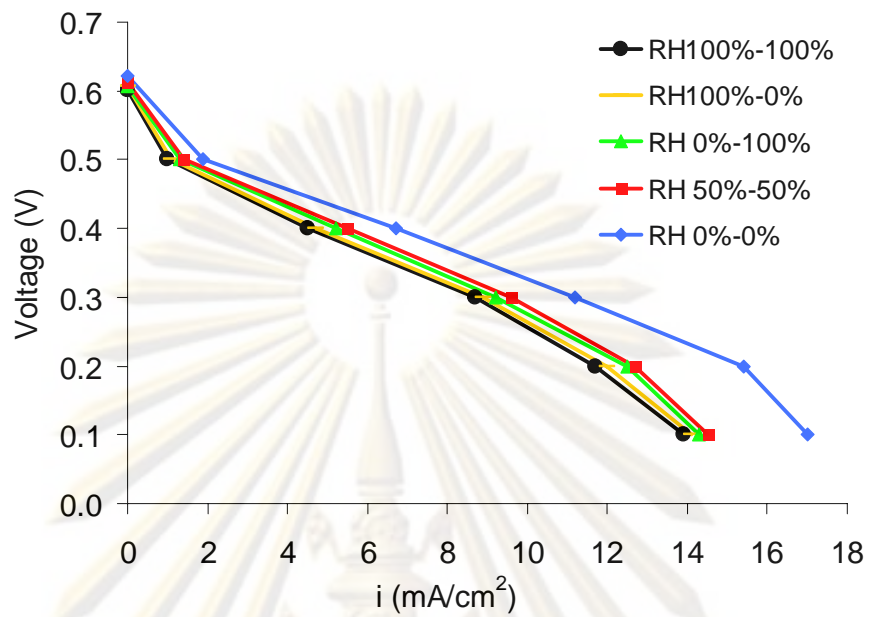


Figure 4.18 Polarization at 30°C of MEA prepared from 30% uncrosslinked chitosan-zeolite membrane at various relative humidity of anode and cathode sides

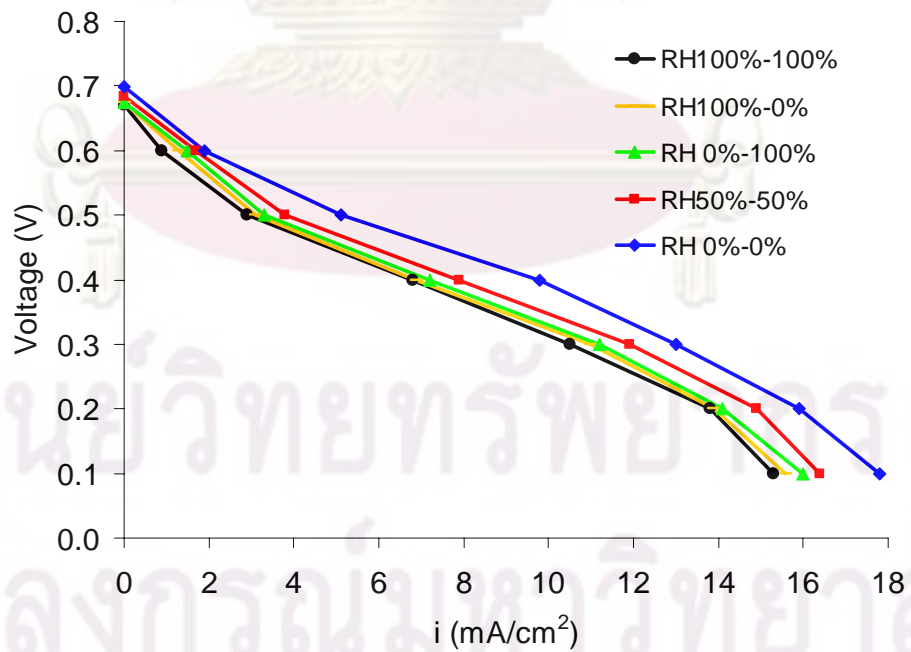


Figure 4.19 Polarization at 30°C of MEA prepared from 30% crosslinked chitosan-zeolite membrane at various relative humidity of anode and cathode sides

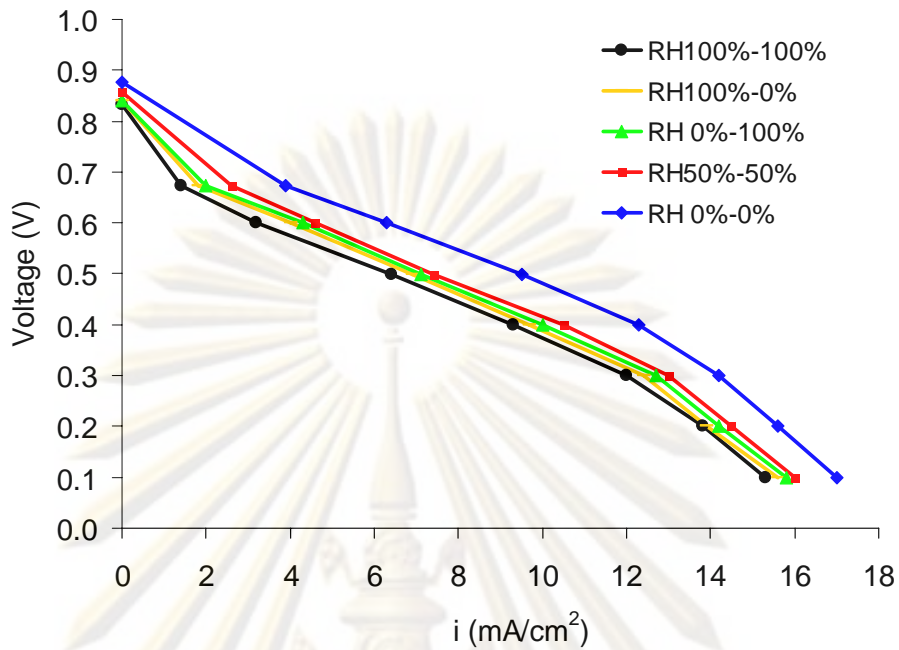


Figure 4.20 Polarization at 30°C of MEA prepared from 30% doped crosslinked chitosan-zeolite membrane at various relative humidity of anode and cathode sides

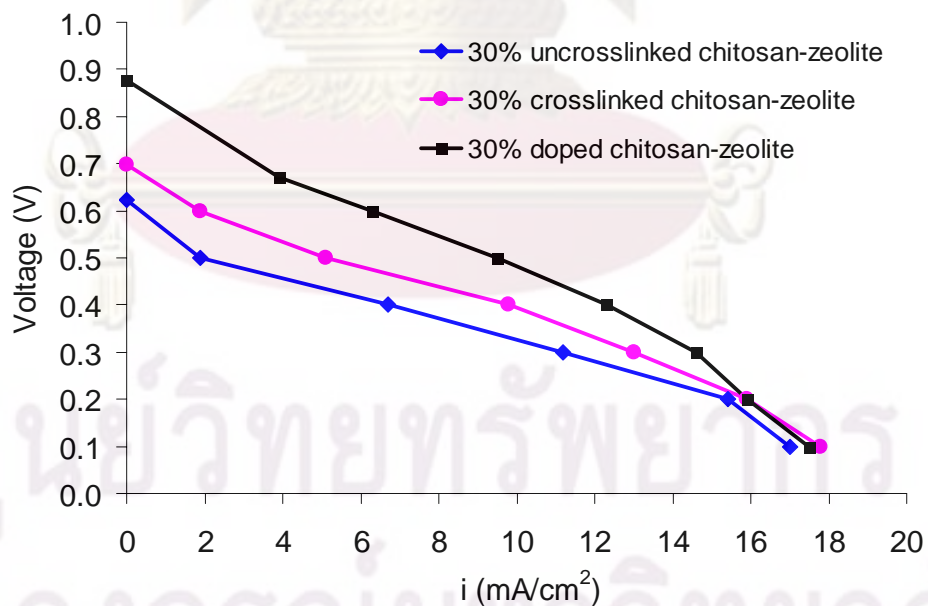


Figure 4.21 Polarization at 30°C of MEA prepared from 30% zeolite contents of uncrosslinked, crosslinked and doped crosslinked chitosan membrane at zero hydration in both anode and cathode sides

The polarization from commercial MEA is shown in Figure 4.22. It showed the opposite sequence to the chitosan based MEA in which the less the humidity of the feed gas especially in the anode side, the worst the performance was. The current density at 0.5 V was increased from 213.2 ± 0.2 for zero hydration (RH 0%-0%) in both sides to 678.1 ± 1.4 mA/cm² at fully hydration (RH 100%-100%). It was not surprising because it was the characteristic of commercial MEA prepared from Nafion membrane. It could be seen that the performance of commercial MEA was much better than that of chitosan based MEA even doped crosslinked chitosan-zeolite MEA. However, it could be stated that we might take an advantage of the hydrophilic chitosan based MEA for the self humidification fuel cell or for high temperature operation.

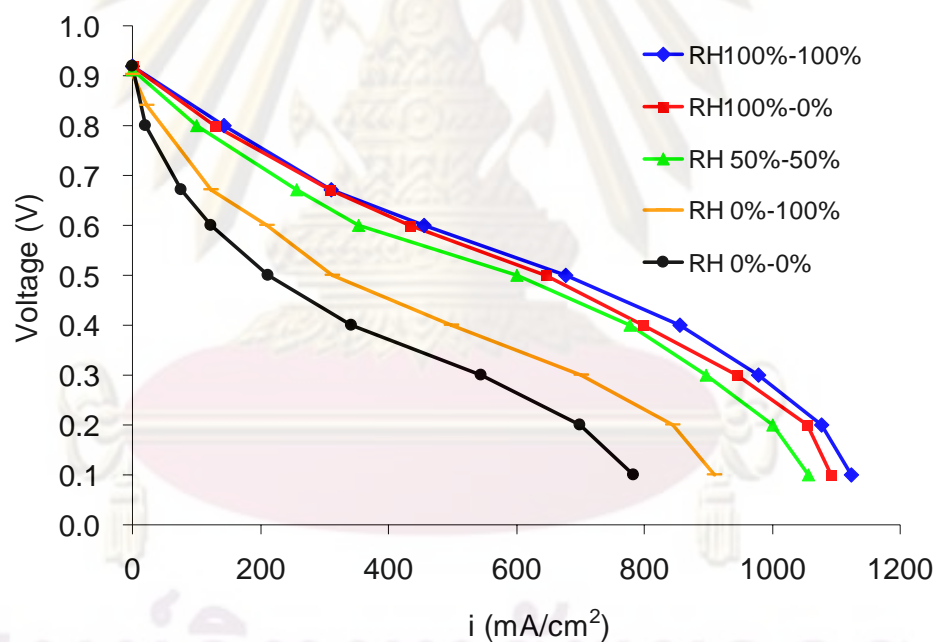


Figure 4.22 Polarization at 30°C of commercial MEA at various relative humidity of anode and cathode sides

The effect of zeolite contents on performance is shown in Figure 4.23 for doped crosslinked chitosan-zeolite MEA at 30°C and zero hydration in both sides. The current density at 0.5 V was increased from 7.1 ± 0.1 to 9.5 ± 0.01 mA/cm² when the zeolite

content was increased from 0 to 30 wt%. The better performance with zeolite contents was also corresponding to the proton conductivity results.

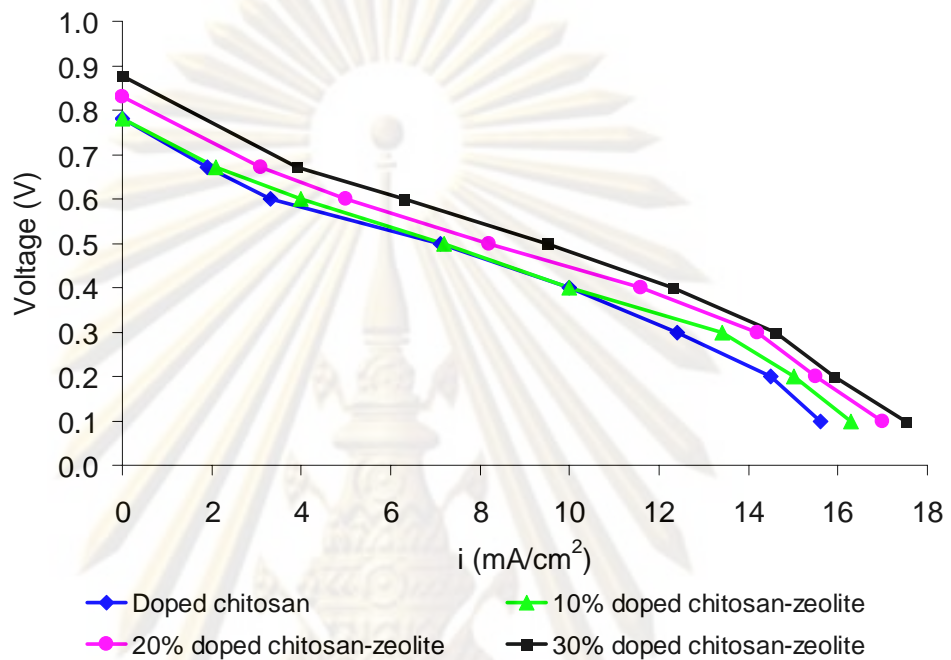


Figure 4.23 Polarization at 30°C of MEA prepared from doped crosslinked chitosan-zeolite membrane for zero hydration in both anode and cathode sides

As shown in Figure 4.24 and 4.25 the performance of 30% doped crosslinked chitosan-zeolite membrane MEA at 60 and 90°C was similar to that of 30°C. The results at zero hydration in both anode and cathode sides are shown together in Figure 4.26, it was shown that the increased temperature enhanced the fuel cell performance as expected. However, the performance at 90°C was not increased respectively. This might be due to the biomaterial effect in notwithstanding the high temperature. The current density at 0.5 V for zero hydration in both anode and cathode sides with a variety of temperatures was increased from 9.5 ± 0.01 to 9.8 ± 0.01 and 10.1 ± 0.01 mA/cm², respectively.

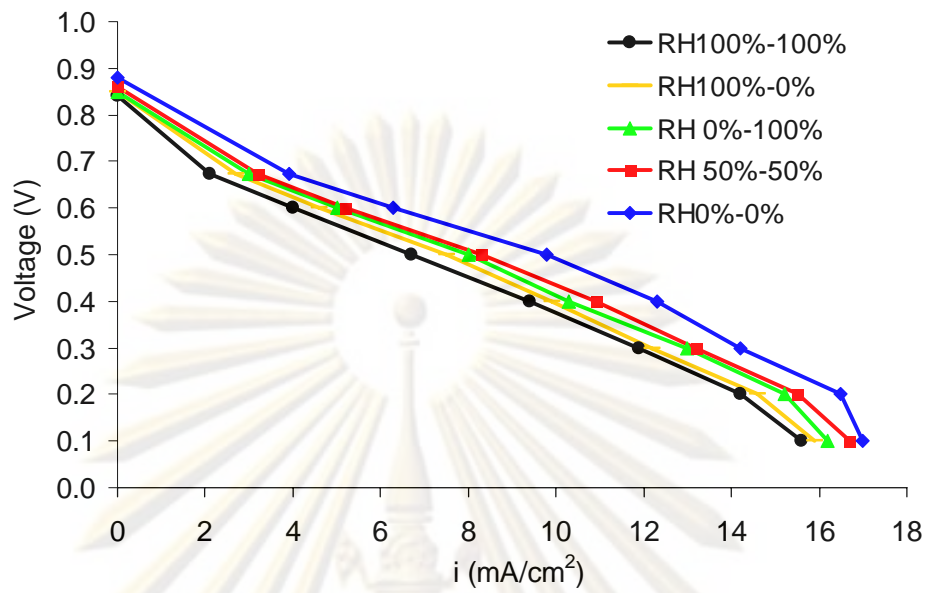


Figure 4.24 Polarization at 60°C of MEA prepared from 30% doped crosslinked chitosan-zeolite membrane at various relative humidity of anode and cathode sides

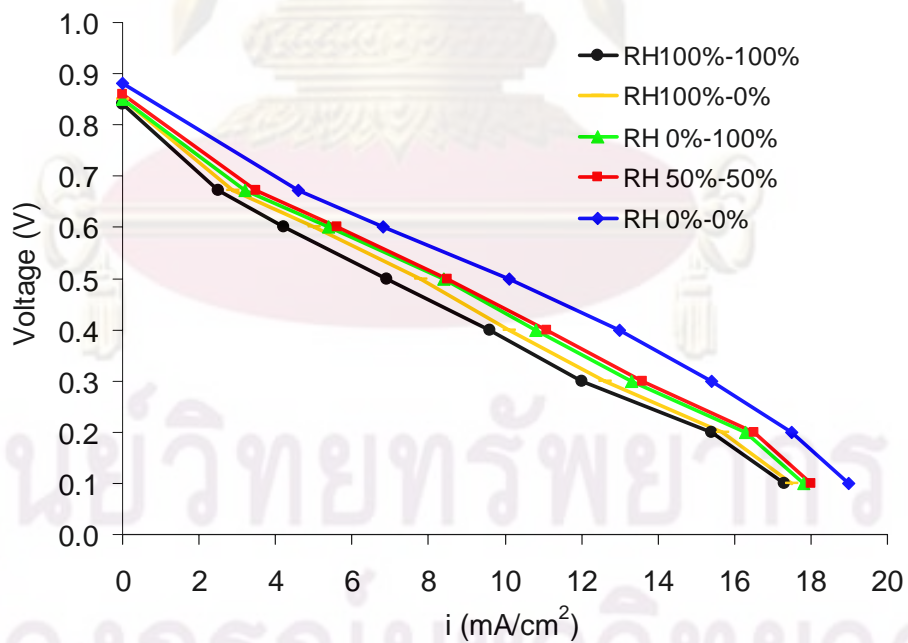


Figure 4.25 Polarization at 90°C of MEA prepared from 30% doped crosslinked chitosan-zeolite membrane at various relative humidity of anode and cathode sides

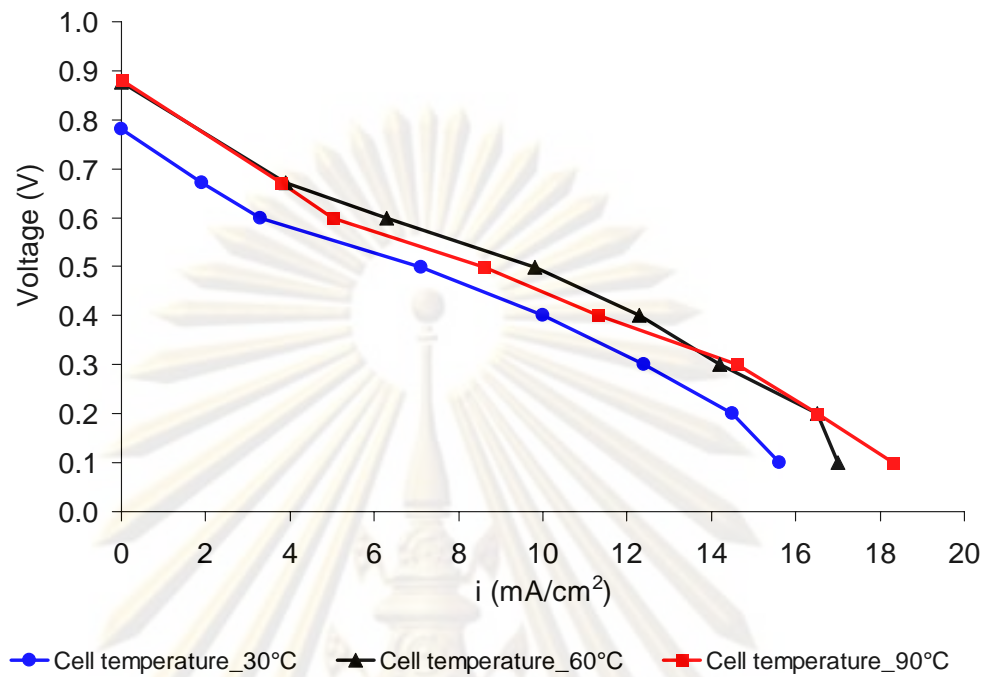


Figure 4.26 Polarization of MEA prepared from 30% doped crosslinked chitosan-zeolite membrane at zero hydration in both anode and cathode sides and various temperatures

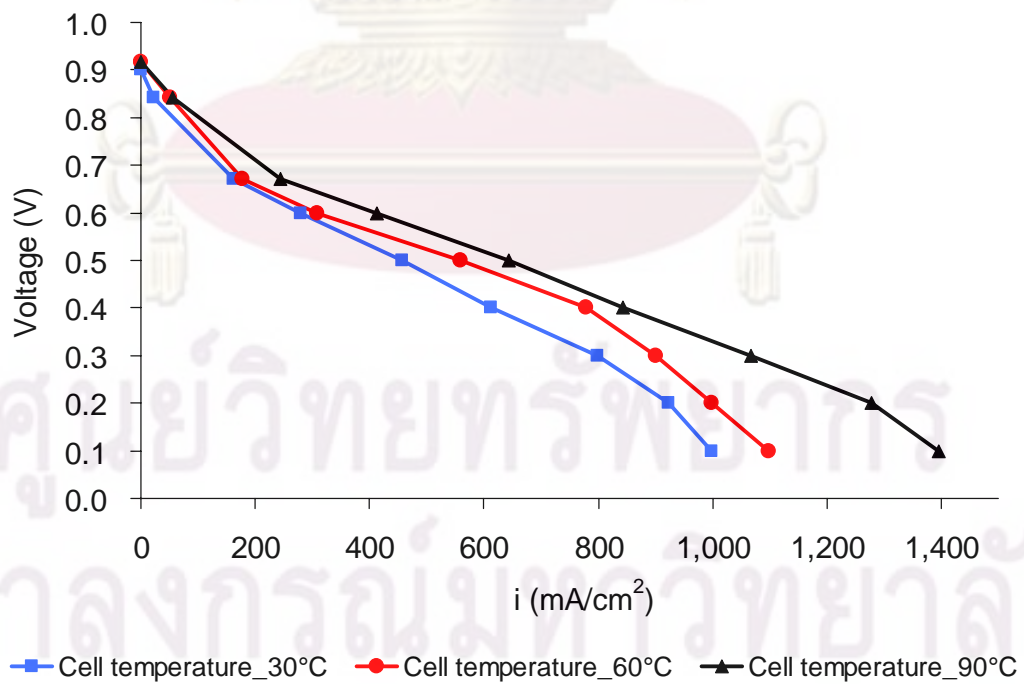
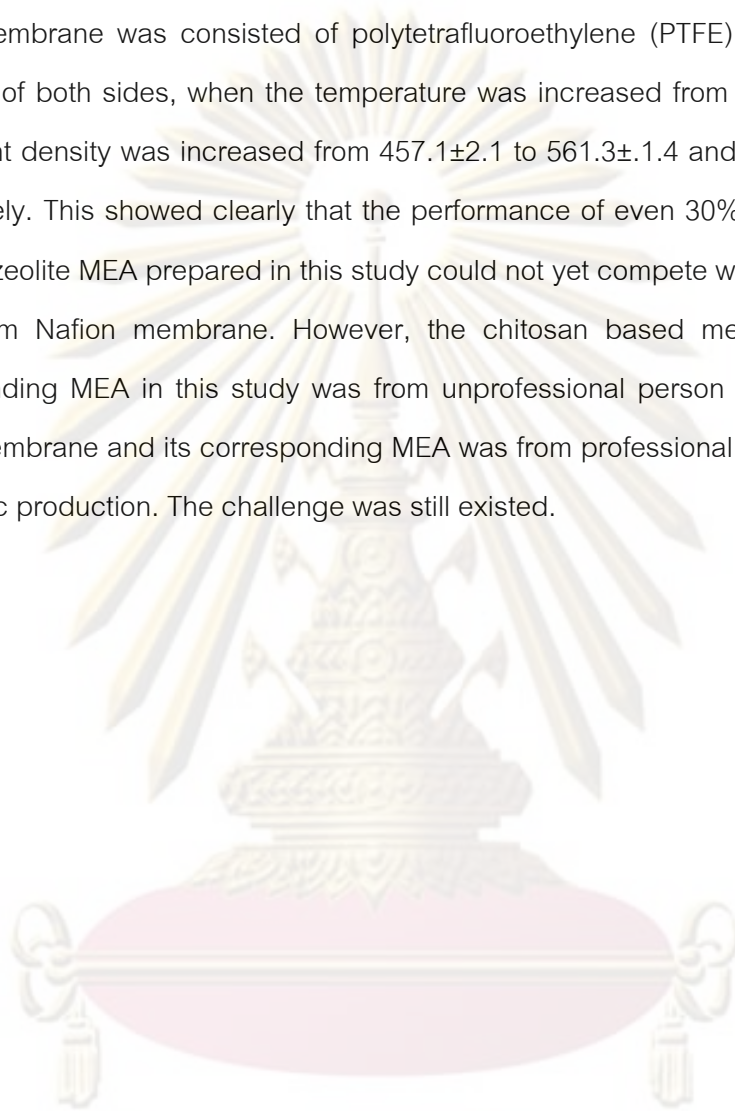


Figure 4.27 Polarization of commercial MEA for zero hydration in both anode and cathode sides at various temperatures

Contrary to the performance from commercial MEA shown in Figure 4.27, the current density was increased with temperature respectively. This was because the Nafion membrane was consisted of polytetrafluoroethylene (PTFE) structures. At zero hydration of both sides, when the temperature was increased from 30 to 60 and 90°C, the current density was increased from 457.1 ± 2.1 to 561.3 ± 1.4 and 643.2 ± 1.4 mA/cm², respectively. This showed clearly that the performance of even 30% doped crosslinked chitosan-zeolite MEA prepared in this study could not yet compete with commercial MEA made from Nafion membrane. However, the chitosan based membranes and their corresponding MEA in this study was from unprofessional person but the commercial Nafion membrane and its corresponding MEA was from professional personnel and from systematic production. The challenge was still existed.



ศูนย์วิจัยทรัพยากร
จุฬาลงกรณ์มหาวิทยาลัย

CHAPTER V

CONCLUSION

5.1 Conclusion

The studied membranes were uncrosslinked chitosan, uncrosslinked chitosan-zeolite, crosslinked chitosan, crosslinked chitosan-zeolite, doped crosslinked chitosan and doped crosslinked chitosan-zeolite membrane.

- Effect of zeolite contents

It was found that the ion exchange capacity and proton conductivity was increased, whilst the tensile strength and H₂ gas permeability was decreased with zeolite content. In single cell testing, the current density was increased with zeolite.

- Effect of temperature

It was found that the H₂ gas permeability and proton conductivity was increased with temperature. The increased temperature enhanced the chemical reactivity and reducing the polarization tremendously yielding better fuel cell performance.

- Effect of doping with 2% by weight of sulfuric acid solution

Although the H₂ gas permeability increased in doped membranes, the proton conductivity and cell performance were the best amongst the studied chitosan based membranes.

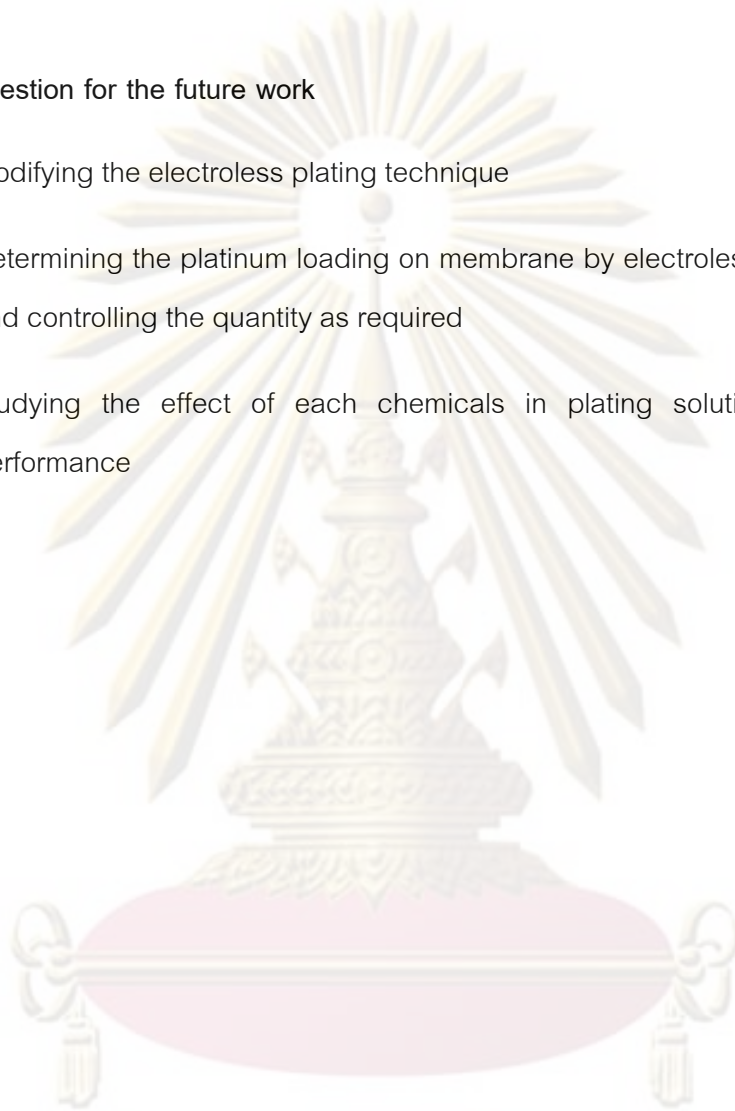
- Effect of humidity on fuel cell performance

The current density at 0.5 V of 30% crosslinked chitosan-zeolite membrane was increased from $2.9 \pm 0.1 \text{ mA/cm}^2$ at fully hydration (RH 100%-100%) to $5.1 \pm 0.1 \text{ mA/cm}^2$ for zero hydration (RH 0%-0%) in both sides and it was increased to $9.5 \pm 0.01 \text{ mA/cm}^2$ in

30% doped crosslinked chitosan-zeolite MEA. Its current density at 60 °C and 90 °C was 9.8 ± 0.01 and 10.1 ± 0.01 mA/cm², respectively.

5.2 Suggestion for the future work

- a) Modifying the electroless plating technique
- b) Determining the platinum loading on membrane by electroless plating technique and controlling the quantity as required
- c) Studying the effect of each chemicals in plating solution on polarization performance



ศูนย์วิทยทรัพยากร
จุฬาลงกรณ์มหาวิทยาลัย

Table 5.1 Properties of 30%crosslinked chitosan-zeolite membrane

Parameter	Non-plated 30% crosslinked chitosan zeolite		Plated 30% crosslinked chitosan zeolite	
	undoped	doped	undoped	doped
Proton Conductivity (S/cm)	0.036±0.002	0.105±0.010	0.212±0.020	0.299±0.005
H ₂ Permeability (barrer)	650±12	1033±52	598±44	987±13
Tensile Strength (MPa)	40.2±0.8	11.6±1.0	-	-
Ion Exchange Capacity (meq/g)	3.71±0.05	-	-	-
Current density (mA/cm ²) at 0.5 V zero hydration and 30°C	-	-	5.1±0.1	9.5±0.01
Current density (mA/cm ²) and 60°C	-	-	5.3±0.2	9.8±0.01
Current density (mA/cm ²) and 90°C	-	-	5.8±0.2	10.1±0.01

References

- [1] Khantong, Soontarapa. Development of Proton Exchange Membrane for Fuel Cell. Bangkok: Department of Chemical Technology, Chulalongkorn University, 2002.
- [2] Unchalee Intra. Preparation and characterization of chitosan composite based proton exchange membrane. Master's Thesis, Department of Chemical Technology, Faculty of Science, Chulalongkorn University, 2003.
- [3] Praphoj Laomongkonnimit. Preparation and characterization of chitosan-zeolite and polysulfone-zeolite protonexchange membrane. Master's Thesis, Department of Chemical Technology, Faculty of Science, Chulalongkorn University, 2005.
- [4] Sirirat Cheryubon. Paladium-coated chitosan/zeolite membrane for PEM fuel cell. Master's Thesis, Department of Chemical Technology, Faculty of Science, Chulalongkorn University, 2008.
- [5] Jutarut Tresuwan. Platinum electroless coating on chitosan based membrane for PEM fuel cell. Master's Thesis, Department of Chemical Technology, Faculty of Science, Chulalongkorn University, 2008.
- [6] Franklin, H. Fuel Cell Test And Evaluation Center [online]. Available from: http://www.fctec.com/fctec_types_afc.asp [2010, Jan 10].
- [7] The Encyclopedia of Alternative Energy and Sustainable. alkaline fuel cell [online]. Available from: http://www.daviddarling.info/encyclopedia/A/AE_alkaline_fuel_cell.html [2010, Jan 10].
- [8] Franklin, H. Fuel Cell Test And Evaluation Center [online]. Available from: http://www.fctec.com/fctec_types_mcfc.asp [2010, Jan 10].
- [9] The Encyclopedia of Alternative Energy and Sustainable. molten carbonate fuel cell [online]. Available from: http://www.daviddarling.info/encyclopedia/M/AE_molten_carbonate_fuel_cell.html [2010, Jan 10].

- [10] Franklin, H. Fuel Cell Test And Evaluation Center [online]. Available from: http://www.fctec.com/fctec_types_softc.asp [2010, Jan 10].
- [11] The Encyclopedia of Alternative Energy and Sustainable. solid oxide fuel cell [online]. Available from: http://www.daviddarling.info/encyclopedia/S/AE_solid_oxide_fuel_cell.html [2010, Jan 10].
- [12] Franklin, H. Fuel Cell Test And Evaluation Center [online]. Available from: http://www.fctec.com/fctec_types_pafc.asp [2010, Jan 10].
- [13] The Encyclopedia of Alternative Energy and Sustainable. phosphoric acid fuel cell [online]. Available from: http://www.daviddarling.info/encyclopedia/P/AE_phosphoric_acid_fuel_cell.html [2010, Jan 10].
- [14] National Science and Technology Development Agency. Ministry of Science and Technology [online]. Available from: http://www.fctec.com/fctec_types_pem.asp [2010, Jan 9].
- [15] Franklin, H. Fuel Cell Test And Evaluation Center [online]. Available from: http://www.fctec.com/fctec_types_pem.asp [2010, Jan 10].
- [16] Broughton, J. fuel cell system. USA: Wikimedia Foundation, 2008.
- [17] Sossina, M. Fuel cell materials and components. Acta Materia. 51 (2003): 5981-6000.
- [18] Nafion® - Perfluorosulfonate Ionomer, Phase Model of Nafion® Clusters [online]. Available from: <http://www.psrc.usm.edu/mauritz/nafion.html> [2010, Jan 2].
- [19] Stephen, V. Current research & development on the PEM fuel cell [online]. Available from: <http://www.fuelcells.org.au/Fuel-Cell-Education-NSW-Australia.htm> [2010, Jan 15].
- [20] Muzzarelli, R.A.A. Chitin. Oxford: Pergamon press, 1977.
- [21] Nishi, N., Maekita, Y., Nishimura, S., Hasegawa, O., and Tokura, S. Highly phosphorylated derivatives of chitin, partially deacetylated chitin and chitosan as new functional polymers: metal binding property of the insolubilized materials. J. Biological Macromolecules 9 (1987): 109-114.

- [22] Sunchanart Sinthawarayun and Somchai Panitchasat. Synthesis of zeolites from coal fly ash. Master's Thesis, Department of Chemical Technology, Faculty of Science, Chulalongkorn University, 1997.
- [23] Abbey Newsletter. Zeolites [online]. Available from: <http://cool.conservation-us.org/byorg/abbey/an/an20/an20-7/an20-702.html> [2010, Jan 15].
- [24] Wang, X. R., Tang, Z. K., and Ge, W. K. Pseudo hysteresis current loop and negative differential resistance in cluster superlattice of tellurium in zeolite. J. Physica B. 271 (1999): 386-395.
- [25] Vielstich, W., Hubert, A., and Gasteiger, A. Handbook of fuel cells – Fundamentals Technology and Applications. 1 st ed. New York: John Wiley & Sons, 2003.
- [26] Larminie, J., and Dick, A. Fuel cell system explained. Chichester: John Wiley, 2000.
- [27] Zawodzinski, T.A., Derouin, C., Radzinski, S., Sherman, R.J., Smith, V.T., Springer, T.E., and Gottesfeld, S. Water uptake by and transport through Nafion 117 membranes. J. Electrochimica Society 140 (1993):1041-1047.
- [28] Yang, B., Fu, Y., and Manthiram, A. Operation of thin Nafion-based self-humidifying membranes in proton exchange membrane fuel cells with dry H₂ and O₂. J. Power Sources 139 (2005): 170–175.
- [29] Ahluwalia, R.K., Doss, E.D., and Kumar, R. Performance of high-temperature polymer electrolyte fuel cell systems. J. Power Sources 117 (2003): 45-60.
- [30] Pitsanu Chalernsombut. A study on ion exchange membrane fuel cell. Master's Thesis, Department of Chemical Technology, Faculty of Science, Chulalongkorn University, 1983.
- [31] Wood, D.L., Yi, J.S., and Nguyen, T.V. Effect of direct liquid water injection and interdigitated flow field on the performance of proton exchange membrane fuel cells. J. Electrochimica Acta 43 (1998): 3795-3809.
- [32] Mc Dougall, A. Fuel cells. 1 st ed. London: The Macmillan Press, 1976.

- [33] Hogarth, W.H.J., and Benziger, J.B. Solid acid membranes for high temperature (>140 °C) proton exchange membrane fuel cells. J. Power Sources 142 (2005): 223–237.
- [34] Apple, A.J., and Foulkes, F.R. Fuel cell handbook. New York: Nostrand Reinhold, 1989.
- [35] Wanwara Huwut. Platinum coating on proton exchange membrane by electroless deposit. Master's Thesis, Department of Chemical Technology, Faculty of Science, Chulalongkorn University, 2004.
- [36] Mukoma, P., Jooste, B.R., and Vosloo, H.C.M. Synthesis and characterization of cross-linked chitosan membranes for application as alternative proton exchange membrane materials in fuel cells. J. Power Sources 136 (2004): 16–23.
- [37] Sun H., Sun G., Wang S., Liu J., et.al., Pd electroless plated Nafion® membrane for high concentration DMFCs. J. Membrane Science 259 (2005): 27–33.
- [38] Watanabe, M., Uchida, H., Seki, Y., Emori, M., and Sbnhart, P. Self-humidifying polymer electrolyte membranes for fuel cells. J. Electrochemical Society 143 (1996): 3847-3852.
- [39] Buchi, F.N., and Srinivasan, S. Operating proton exchange membrane fuel cells without external humidification of the reactant gases. J. Electrochemical Society 144 (1997): 2767-2772.
- [40] Andraeus, B., Mc Evoy, A.J., and Scherer, G.G. Analysis of performance losses in polymer electrolyte fuel cells at high current densities by impedance spectroscopy. J. Electrochimica Acta 47 (2001): 2223-2229.
- [41] Chompoonoot Ussaratnivas. Preparation and characterization of chitosan/zeolite membrane for separation of CH₄ in biogas. Master's Thesis, Department of Chemical Technology, Faculty of Science, Chulalongkorn University, 2008.
- [42] Pram Yodjun. Separation of lycopene/solvent mixtures by chitosan by chitosan membranes. Master's Thesis, Department of Chemical Technology, Faculty of Science, Chulalongkorn University, 2009



APPENDICES

ศูนย์วิทยทรัพยากร
จุฬาลงกรณ์มหาวิทยาลัย

APPENDIX A

Data

Table A-1 Tensile strength

Type of membranes	Tensile strength (MPa)
Uncrosslinked chitosan	50±1.76
Uncrosslinked chitosan-zeolite 10%	36.3±1.05
Uncrosslinked chitosan-zeolite 20%	29.3±1.30
Uncrosslinked chitosan-zeolite 30%	19.6±1.15
Crosslinked chitosan	62.5±0.86
Crosslinked chitosan-zeolite 10%	60±1.29
Crosslinked chitosan-zeolite 20%	57.3±1.98
Crosslinked chitosan-zeolite 30%	40.2±0.75
Doped chitosan	29.6±1.15
Doped chitosan-zeolite 10%	15.7±0.47
Doped chitosan-zeolite 20%	13.8±0.95
Doped chitosan-zeolite 30%	11.6±0.95
Nafion	28.4±0.30

ศูนย์วิทยทรัพยากร
จุฬาลงกรณ์มหาวิทยาลัย

Table A-2. Gas permeability at 30 °C

Type of membranes	Hydrogen permeability (Barrer)
Uncrosslinked chitosan	1300±1.66
Uncrosslinked chitosan-zeolite 10%	1100±1.02
Uncrosslinked chitosan-zeolite 20%	1000±1.50
Uncrosslinked chitosan-zeolite 30%	800±1.25
Crosslinked chitosan	1000±0.96
Crosslinked chitosan-zeolite 10%	850±1.21
Crosslinked chitosan-zeolite 20%	700±1.78
Crosslinked chitosan-zeolite 30%	650±0.65
Doped chitosan	1600±1.05
Doped chitosan-zeolite 10%	1400±0.42
Doped chitosan-zeolite 20%	1289±0.91
Doped chitosan-zeolite 30%	1033±0.35
Nafion	6100±0.20

ศูนย์วิทยทรัพยากร
จุฬาลงกรณ์มหาวิทยาลัย

Table A-3. Gas permeability at 60 °C

Type of membranes	Hydrogen permeability (Barrer)
Uncrosslinked chitosan	1450±1.62
Uncrosslinked chitosan-zeolite 10%	1400±1.00
Uncrosslinked chitosan-zeolite 20%	1290±1.31
Uncrosslinked chitosan-zeolite 30%	900±1.22
Crosslinked chitosan	1200±0.46
Crosslinked chitosan-zeolite 10%	980±1.20
Crosslinked chitosan-zeolite 20%	810±1.21
Crosslinked chitosan-zeolite 30%	790±0.64
Doped chitosan	1800±1.20
Doped chitosan-zeolite 10%	1690±0.10
Doped chitosan-zeolite 20%	1340±0.01
Doped chitosan-zeolite 30%	1230±0.32
Nafion	6900±0.22

ศูนย์วิทยทรัพยากร
จุฬาลงกรณ์มหาวิทยาลัย

Table A-4 Gas permeability at 90 °C

Type of membranes	Hydrogen permeability (Barrer)
Uncrosslinked chitosan	1670±1.32
Uncrosslinked chitosan-zeolite 10%	1780±1.19
Uncrosslinked chitosan-zeolite 20%	1340±1.03
Uncrosslinked chitosan-zeolite 30%	1000±1.25
Crosslinked chitosan	1350±0.50
Crosslinked chitosan-zeolite 10%	1100±1.20
Crosslinked chitosan-zeolite 20%	990±1.25
Crosslinked chitosan-zeolite 30%	987±0.60
Doped chitosan	2100±1.20
Doped chitosan-zeolite 10%	1795±0.06
Doped chitosan-zeolite 20%	1496±0.40
Doped chitosan-zeolite 30%	1340±0.34
Nafion	7300±0.69

Table A-5 Ion exchange capacity

Type of membranes	Ion exchange capacity (meq/g)
Crosslinked chitosan	3.43±0.05
Crosslinked chitosan-zeolite 10%	3.64±0.05
Crosslinked chitosan-zeolite 20%	3.68±0.10
Crosslinked chitosan-zeolite 30%	3.71±0.05
Nafion	1.32±0.50

ศูนย์วิทยทรัพยากร
จุฬาลงกรณ์มหาวิทยาลัย

Table A-6 Proton conductivity at 30 °C in planar view

Type of membranes	Proton conductivity (S/cm)
Uncrosslinked chitosan	0.007±0.001
Uncrosslinked chitosan-zeolite 10%	0.010±0.001
Uncrosslinked chitosan-zeolite 20%	0.013±0.002
Uncrosslinked chitosan-zeolite 30%	0.017±0.004
Crosslinked chitosan	0.011±0.003
Crosslinked chitosan-zeolite 10%	0.016±0.007
Crosslinked chitosan-zeolite 20%	0.030±0.009
Crosslinked chitosan-zeolite 30%	0.036±0.002
Doped chitosan	0.070±0.011
Doped chitosan-zeolite 10%	0.082±0.015
Doped chitosan-zeolite 20%	0.099±0.015
Doped chitosan-zeolite 30%	0.105±0.010
Nafion	0.057±0.005

ศูนย์วิทยทรัพยากร
จุฬาลงกรณ์มหาวิทยาลัย

Table A-7 Proton conductivity at 60 °C

Type of membranes	Proton conductivity (S/cm)
Uncrosslinked chitosan	0.010±0.002
Uncrosslinked chitosan-zeolite 10%	0.015±0.004
Uncrosslinked chitosan-zeolite 20%	0.018±0.002
Uncrosslinked chitosan-zeolite 30%	0.021±0.003
Crosslinked chitosan	0.012±0.004
Crosslinked chitosan-zeolite 10%	0.019±0.003
Crosslinked chitosan-zeolite 20%	0.035±0.006
Crosslinked chitosan-zeolite 30%	0.043±0.006
Doped chitosan	0.082±0.015
Doped chitosan-zeolite 10%	0.090±0.011
Doped chitosan-zeolite 20%	0.109±0.009
Doped chitosan-zeolite 30%	0.123±0.024
Nafion	0.069±0.004

ศูนย์วิทยทรัพยากร
จุฬาลงกรณ์มหาวิทยาลัย

Table A-8 Proton conductivity at 90 °C

Type of membranes	Proton conductivity (S/cm)
Uncrosslinked chitosan	0.013±0.002
Uncrosslinked chitosan-zeolite 10%	0.020±0.007
Uncrosslinked chitosan-zeolite 20%	0.022±0.004
Uncrosslinked chitosan-zeolite 30%	0.025±0.003
Crosslinked chitosan	0.018±0.008
Crosslinked chitosan-zeolite 10%	0.025±0.009
Crosslinked chitosan-zeolite 20%	0.043±0.005
Crosslinked chitosan-zeolite 30%	0.047±0.006
Doped chitosan	0.100±0.009
Doped chitosan-zeolite 10%	0.110±0.033
Doped chitosan-zeolite 20%	0.123±0.024
Doped chitosan-zeolite 30%	0.130±0.020
Nafion	0.072±0.002

ศูนย์วิทยทรัพยากร
จุฬาลงกรณ์มหาวิทยาลัย

Table A-9 Proton conductivity at 30°C after Pt plating by electroless technique at 60°C for 90 min in planar view

Type of membranes	Proton conductivity (S/cm)
Uncrosslinked chitosan	0.028±0.009
Uncrosslinked chitosan-zeolite 10%	0.041±0.009
Uncrosslinked chitosan-zeolite 20%	0.070±0.009
Uncrosslinked chitosan-zeolite 30%	0.108±0.029
Crosslinked chitosan	0.137±0.010
Crosslinked chitosan-zeolite 10%	0.159±0.026
Crosslinked chitosan-zeolite 20%	0.176±0.017
Crosslinked chitosan-zeolite 30%	0.212±0.020
Doped chitosan	0.235±0.019
Doped chitosan-zeolite 10%	0.257±0.006
Doped chitosan-zeolite 20%	0.281±0.012
Doped chitosan-zeolite 30%	0.299±0.005

ศูนย์วิทยทรัพยากร
จุฬาลงกรณ์มหาวิทยาลัย

Table A-10 Proton conductivity at 60°C after Pt plating by electroless technique

Type of membranes	Proton conductivity (S/cm)
Uncrosslinked chitosan	0.093±0.005
Uncrosslinked chitosan-zeolite 10%	0.105±0.023
Uncrosslinked chitosan-zeolite 20%	0.130±0.009
Uncrosslinked chitosan-zeolite 30%	0.150±0.006
Crosslinked chitosan	0.149±0.029
Crosslinked chitosan-zeolite 10%	0.183±0.008
Crosslinked chitosan-zeolite 20%	0.207±0.021
Crosslinked chitosan-zeolite 30%	0.235±0.003
Doped chitosan	0.255±0.017
Doped chitosan-zeolite 10%	0.278±0.013
Doped chitosan-zeolite 20%	0.293±0.006
Doped chitosan-zeolite 30%	0.312±0.008

ศูนย์วิทยทรัพยากร
จุฬาลงกรณ์มหาวิทยาลัย

Table A-11 Proton conductivity at 90°C after Pt plating by electroless technique

Type of membranes	Proton conductivity (S/cm)
Uncrosslinked chitosan	0.097±0.010
Uncrosslinked chitosan-zeolite 10%	0.129±0.010
Uncrosslinked chitosan-zeolite 20%	0.152±0.003
Uncrosslinked chitosan-zeolite 30%	0.184±0.008
Crosslinked chitosan	0.153±0.001
Crosslinked chitosan-zeolite 10%	0.197±0.005
Crosslinked chitosan-zeolite 20%	0.221±0.004
Crosslinked chitosan-zeolite 30%	0.240±0.009
Doped chitosan	0.270±0.011
Doped chitosan-zeolite 10%	0.301±0.008
Doped chitosan-zeolite 20%	0.344±0.009
Doped chitosan-zeolite 30%	0.357±0.007

ศูนย์วิทยทรัพยากร
จุฬาลงกรณ์มหาวิทยาลัย

Table A-12 Gas permeability of 30% crosslinked chitosan-zeolite membranes after Pt plating by electroless technique in condition dry gas and membranes

Temperature (°C)	Hydrogen permeability (Barrer)
30	660±1.22
60	800±1.10
90	900±1.08

Table A-13 Gas permeability in condition humid gas and dry membranes

Temperature (°C)	Hydrogen permeability (Barrer)
30	980±1.29
60	1100±1.00
90	1200±1.56

Table A-14 Gas permeability in condition humid gas and membranes

Temperature (°C)	Hydrogen permeability (Barrer)
30	1450±1.32
60	1600±1.19
90	1700±1.03

ศูนย์วิทยทรัพยากร
จุฬาลงกรณ์มหาวิทยาลัย

Table A-15 Proton conductivity of MEA at 30 °C in cross section view

Type of membranes	Proton conductivity (S/cm)
Uncrosslinked chitosan	0.001±0.004
Uncrosslinked chitosan-zeolite 10%	0.002±0.001
Uncrosslinked chitosan-zeolite 20%	0.003±0.002
Uncrosslinked chitosan-zeolite 30%	0.005±0.004
Crosslinked chitosan	0.002±0.003
Crosslinked chitosan-zeolite 10%	0.004±0.001
Crosslinked chitosan-zeolite 20%	0.006±0.009
Crosslinked chitosan-zeolite 30%	0.009±0.002
Doped chitosan	0.018±0.011
Doped chitosan-zeolite 10%	0.024±0.015
Doped chitosan-zeolite 20%	0.031±0.015
Doped chitosan-zeolite 30%	0.035±0.010

ศูนย์วิทยทรัพยากร
จุฬาลงกรณ์มหาวิทยาลัย

Table A-16 Proton conductivity of MEA at 60 °C

Type of membranes	Proton conductivity (S/cm)
Uncrosslinked chitosan	0.003±0.003
Uncrosslinked chitosan-zeolite 10%	0.006±0.007
Uncrosslinked chitosan-zeolite 20%	0.009±0.002
Uncrosslinked chitosan-zeolite 30%	0.013±0.002
Crosslinked chitosan	0.004±0.004
Crosslinked chitosan-zeolite 10%	0.008±0.006
Crosslinked chitosan-zeolite 20%	0.011±0.002
Crosslinked chitosan-zeolite 30%	0.016±0.002
Doped chitosan	0.024±0.003
Doped chitosan-zeolite 10%	0.030±0.005
Doped chitosan-zeolite 20%	0.032±0.009
Doped chitosan-zeolite 30%	0.040±0.010

ศูนย์วิทยทรัพยากร
จุฬาลงกรณ์มหาวิทยาลัย

Table A-17 Proton conductivity of MEA at 90 °C

Type of membranes	Proton conductivity (S/cm)
Uncrosslinked chitosan	0.005±0.002
Uncrosslinked chitosan-zeolite 10%	0.008±0.003
Uncrosslinked chitosan-zeolite 20%	0.014±0.006
Uncrosslinked chitosan-zeolite 30%	0.018±0.004
Crosslinked chitosan	0.008±0.004
Crosslinked chitosan-zeolite 10%	0.010±0.007
Crosslinked chitosan-zeolite 20%	0.015±0.005
Crosslinked chitosan-zeolite 30%	0.019±0.001
Doped chitosan	0.029±0.009
Doped chitosan-zeolite 10%	0.037±0.003
Doped chitosan-zeolite 20%	0.041±0.006
Doped chitosan-zeolite 30%	0.048±0.010

ศูนย์วิทยทรัพยากร
จุฬาลงกรณ์มหาวิทยาลัย

Table A-18 The current density at 0.5 V of 30% uncrosslinked chitosan-zeolite membranes, cell temperature 30°C

% Relative humidity (anode-cathode)	Current density (mA/cm ²)
100-100	1.000±0.070
100-0	1.100±0.070
0-100	1.300±0.080
50-50	1.400±0.282
0-0	1.500±0.141

Table A-19 The current density at 0.5 V of 30% crosslinked chitosan-zeolite membranes

% Relative humidity (anode-cathode)	Current density (mA/cm ²)
100-100	2.900±0.141
100-0	3.100±0.070
0-100	3.300±0.101
50-50	3.800±0.282
0-0	5.100±0.141

Table A-20 The current density at 0.5 V of 30% doped chitosan-zeolite membranes

% Relative humidity (anode-cathode)	Current density (mA/cm ²)
100-100	6.400±0.007
100-0	6.900±0.141
0-100	7.100±0.006
50-50	7.400±0.424
0-0	9.500±0.009

Table A-21 The current density at 0.5 V of doped chitosan-zeolite membranes at zero hydration of anode and cathode sides

% Zeolite by weight of chitosan	Current density (mA/cm ²)
0	7.100±0.141
10	7.200±0.282
20	8.200±0.282
30	9.500±0.009

Table A-22 The current density at 0.5 V of 30% uncrosslinked chitosan-zeolite membranes, cell temperature 60°C

% Relative humidity (anode-cathode)	Current density (mA/cm ²)
100-100	1.800±0.287
100-0	1.900±0.070
0-100	2.100±0.070
50-50	2.200±0.075
0-0	2.900±0.141

Table A-23 The current density at 0.5 V of 30% crosslinked chitosan-zeolite membranes

% Relative humidity (anode-cathode)	Current density (mA/cm ²)
100-100	4.000±0.141
100-0	4.300±0.149
0-100	4.500±0.140
50-50	4.900±0.145
0-0	5.300±0.147

Table A-24 The current density at 0.5 V of 30% doped chitosan-zeolite membranes

% Relative humidity (anode-cathode)	Current density (mA/cm ²)
100-100	6.700±0.004
100-0	7.500±0.141
0-100	8.000±0.141
50-50	8.300±0.424
0-0	9.800±0.007

Table A-25 The current density at 0.5 V of 30% uncrosslinked chitosan-zeolite membranes, cell temperature 90°C

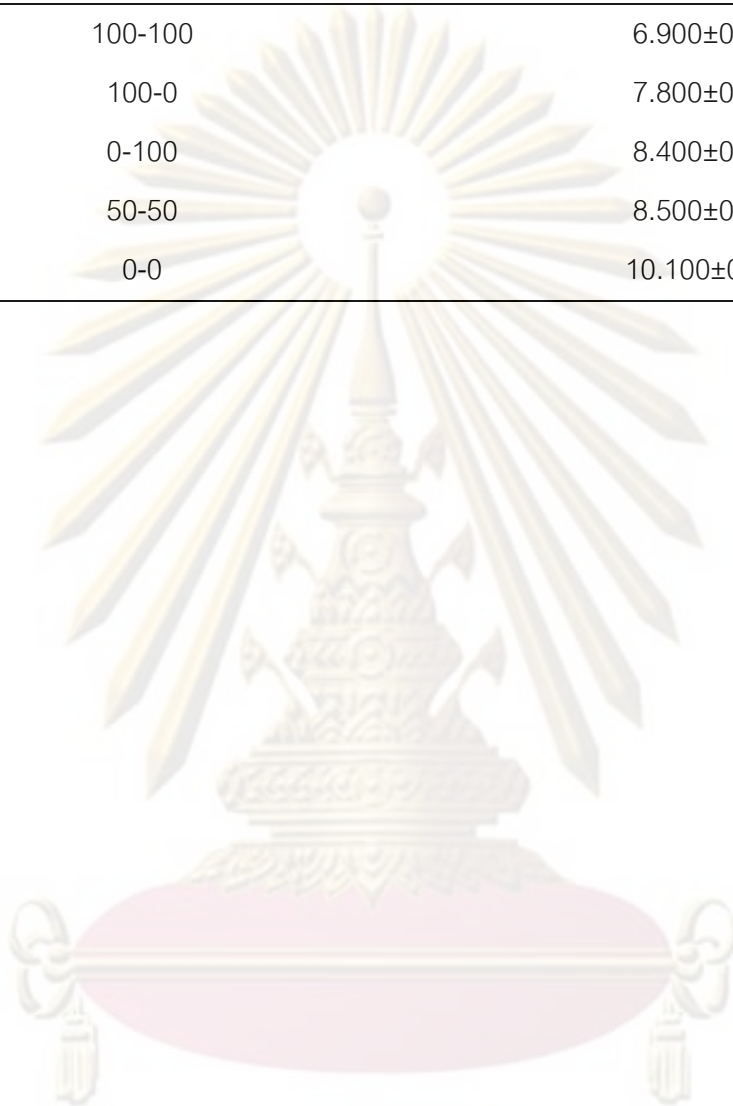
% Relative humidity (anode-cathode)	Current density (mA/cm ²)
100-100	1.900±0.287
100-0	2.100±0.070
0-100	2.300±0.070
50-50	2.400±0.075
0-0	3.100±0.141

Table A-26 The current density at 0.5 V of 30% crosslinked chitosan-zeolite membranes

% Relative humidity (anode-cathode)	Current density (mA/cm ²)
100-100	4.200±0.141
100-0	4.500±0.149
0-100	4.900±0.149
50-50	5.500±0.141
0-0	5.800±0.242

Table A-27 The current density at 0.5 V of 30% doped chitosan-zeolite membranes

% Relative humidity (anode-cathode)	Current density (mA/cm ²)
100-100	6.900±0.004
100-0	7.800±0.141
0-100	8.400±0.141
50-50	8.500±0.424
0-0	10.100±0.007



ศูนย์วิทยทรัพยากร
จุฬาลงกรณ์มหาวิทยาลัย

APPENDIX B
Example calculation

1. Gas permeability

Flow rate of permeated hydrogen gas	= 0.0156 (Sccs)
Diameter	= 3.20 cm
Membrane thickness	= 0.019 (cm)
Pressure difference	= 77.0070 (cmHg)
membrane surface area	= 8.0457 cm ²

$$P = \frac{QL}{\Delta PA}$$

P = Permeability coefficient (cm³ (STP)*cm)/(s*cm²*cmHg)

Q = Flow rate of permeated hydrogen gas (Sccs)

L = Membrane thickness (cm)

ΔP = Pressure difference (cmHg)

A = Surface area of membrane (cm²)

$$P = \frac{0.0156 \times 0.019}{77.0070 \times 8.0457}$$

$$= 4.89 \times 10^{-7} \text{ (cm}^3 \text{ (STP)*cm)/(s*cm}^2 \text{*Hg)}$$

$$= 4899.5 \text{ barrer}$$

$$1 \text{ Barrer} = 10^{-10} \text{ (cm}^3 \text{ (STP)*cm)/(s*cm}^2 \text{*Hg)}$$

2. Ion exchange capacity

Concentration of NaOH solution	= 0.005 (N)
Concentration of HCl acid	= 0.005 (N)
Volume of NaOH	= 22 (ml)
Volume of HCl	= 1.8 (ml)
Volume of NaOH used for titration	= 10 (ml)
Weight of membrane	= 0.0202 (g.)

$$\text{Ion exchange capacity} = \frac{\left(N_1 V_1 - \left(\frac{V_1}{V_3} \right) N_2 V_2 \right)}{m}$$

N_1 = Concentration of NaOH solution (N)

N_2 = Concentration of HCl acid (N)

V_1 = Volume of NaOH (ml)

V_2 = Volume of HCl (ml)

V_3 = Volume of NaOH used for titration (ml)

m = Weight of membrane (g.)

$$\text{Ion exchange capacity} = \frac{(0.005 \times 22) - \left(\frac{22}{10} \times 0.005 \times 1.8 \right)}{0.0202}$$

$$= 4.46 \text{ meq/g}$$

ศูนย์วิทยาศาสตร์

จุฬาลงกรณ์มหาวิทยาลัย

3. Proton conductivity in planar view

Membrane thickness	= 0.0020 cm
Membrane width	= 1 cm
Resistivity (Ohm)	= 20,056 (Ohm)
Distance between the platinum electrodes	= 0.5 (cm)
Cross-section area of membrane	= 0.0020

$$\sigma = \frac{1}{R} \left(\frac{L}{A} \right)$$

σ	=	Proton conductivity (Siemens/cm)
R	=	Resistivity (Ohm)
L	=	Distance between the platinum electrodes (cm)
A	=	Cross-section area of membrane cm ²

$$\sigma = \frac{1 \times 0.5}{20,056 \times 0.0020}$$

$$= 0.0124 \text{ (Siemens/cm)}$$

ศูนย์วิทยทรัพยากร
จุฬาลงกรณ์มหาวิทยาลัย

4. Proton conductivity in cross section view

MEA thickness (cm)	= 0.0520
MEA width	= 0.0520 cm
Resistivity	= 563 (Ohm)
Surface area of MEA	2.3×2.3 = 5.29 cm ²
Thickness of MEA	= 0.0520 (cm)

$$\sigma = \frac{1}{R} \left(\frac{L}{A} \right)$$

σ	=	Proton conductivity (Siemens/cm)
R	=	Resistivity (Ohm)
L	=	Thickness of MEA (cm)
A	=	Cross section of membrane (cm ²)

$$\sigma = \frac{1 \times 0.052}{563 \times 5.29}$$

$$= 1.74 \times 10^{-5} \text{ (Siemens/cm)}$$

ศูนย์วิทยทรัพยากร
จุฬาลงกรณ์มหาวิทยาลัย

VITAE

Miss. Agkarapin Angkatreerat was born on March 17, 1985 in Buriram, Thailand. She graduated with Bachelor Degree of Science in General Science From Chulalongkorn University in 2007. Since then, she has been a graduate student studying Petrochemistry and Polymer Science at Chulalongkorn University. She was supported by research grant for this Master Degree's thesis from the National Center of Excellence for Petroleum, Petrochemicals, and Advanced Materials, NCE-PPAM, the Thailand Research Fund and the 90th Anniversary of chulalongkorn university fund (Ratchadaphiseksomphot Endowment Fund).

Presentation Experience

Oral presentation from Pure and Applied Chemistry International Conference 2010 in the topic of "EFFECTS OF RELATIVE HUMIDITY ON PERFORMANCE OF Pt/ZEOILITE-CHITOSAN MEMBRANE IN PEM FUEL CELL" on 22 January 2553 at Ubonratchathani University.

ศูนย์วิทยทรัพยากร
จุฬาลงกรณ์มหาวิทยาลัย